

Noise-Reuse in Online Evolution Strategies

Oscar Li^{§*}, James Harrison[◇], Jascha Sohl-Dickstein[◇], Virginia Smith[§], Luke Metz^{◇†}

[§]Machine Learning Department, School of Computer Science Carnegie Mellon University

[◇]Google Research, Brain Team

Abstract

Online evolution strategies have become an attractive alternative to automatic differentiation (AD) due to their ability to handle chaotic and black-box loss functions, while also allowing more frequent gradient updates than vanilla Evolution Strategies (ES). In this work, we propose a general class of unbiased online evolution strategies. We analytically and empirically characterize the variance of this class of gradient estimators and identify the one with the least variance, which we term Noise-Reuse Evolution Strategies (NRES). Experimentally, we show that NRES results in faster convergence than existing AD and ES methods in terms of wall-clock speed and total number of unroll steps across a variety of applications, including learning dynamical systems, meta-training learned optimizers, and reinforcement learning.

1 Introduction

First-order optimization methods are a foundational tool in machine learning. With many such methods (e.g., SGD, Adagrad, Adam) readily available and implemented in existing software, ML training often amounts to specifying a computation graph of learnable parameters and computing some notion of gradients to pass into an off-the-shelf optimizer. Here, *unrolled computation graphs* (UCGs), where the same learnable parameters are repeatedly used to transition a dynamical system’s inner state, have found their use in various applications such as recurrent neural networks [Hochreiter and Schmidhuber, 1997], meta-training learned optimizers [Metz et al., 2019], hyperparameter-tuning [Maclaurin et al., 2015], dataset distillation [Wang et al., 2018], and reinforcement learning [Sutton et al., 1999].

Despite the existence of a large number of automatic differentiation (AD) techniques to estimate gradients in UCGs [Baydin et al., 2018], such methods are known to perform poorly with chaotic or poorly conditioned loss landscapes and are unable to handle black-box computation dynamics or discontinuous losses [Metz et al., 2019]. To handle these shortcomings, evolution strategies (ES) have become an effective alternative to produce gradient estimates in UCGs [Salimans et al., 2017]. ES convolves the (potentially chaotic or discontinuous) loss surface with a Gaussian distribution in the parameter space, making it smoother and infinitely differentiable. Unfortunately, without taking into consideration the successive nature of unrolled computation graphs, the vanilla ES methods cannot be applied online¹ and the computation must reach the end of the graph to obtain an update. To address this, a recently proposed approach, Persistent Evolution Strategies [Vicol et al., 2021] (PES), reduces the latency of gradient updates while producing an unbiased

*Correspondence to: Oscar Li <oscarli@cmu.edu>

†Now at OpenAI.

¹Online in this paper means one can obtain gradient estimates using only a *truncation window* of an unrolled computation graph *instead of the full graph*, thus allowing the interleaving of partial unrolls and parameter updates.

estimate of a surrogate stochastic computation graph by accumulating the noise sampled in past truncation windows.

In this work, we investigate the coupling of the noise sampling frequency and the gradient estimation frequency in the online ES method PES. By uncoupling these two frequencies, we arrive at a more general class of unbiased, online ES gradient estimators. Through a variance characterization of these estimators, we find that the one that provably has the lowest variance (and thus lower variance than PES) in fact reuses the same noise for the entire time horizon (instead of over a single truncation window as in PES). We call this method Noise-Reuse Evolution Strategies (NRES). In addition to being simple to implement, we show that NRES can converge faster than PES across a wide variety of applications due to its reduced variance.

Overall, we make the following contributions:

- We propose a class of unbiased online Evolution Strategies gradient estimators for unrolled computation graphs that generalize (and include) Persistent Evolution Strategies.
- We characterize the variance of this class of estimators, and identify the lowest-variance estimator within the class. We term this estimator Noise Reuse Evolution Strategies (NRES) due to its noise sharing properties².
- We empirically show the variance advantage of NRES over other estimators in our newly proposed class.
- We demonstrate the convergence benefits of NRES over AD/ES baselines in terms of wall-clock speed and number of unroll steps in applications of 1) parameter identification in dynamical systems, 2) meta-training learned optimizers, and 3) reinforcement learning. We provide a JAX [Bradbury et al., 2018] implementation of all the algorithms and applications³.

2 Background

Problem setup. Unrolled computation graphs (UCGs) are commonly encountered in applications such as training recurrent neural networks, meta-training learned optimizers, and learning policies in reinforcement learning, where the same set of parameters are repeatedly used to update the inner state of some system. We consider general UCGs where the inner state $s_t \in \mathbb{R}^p$ is updated with learnable parameter $\theta \in \mathbb{R}^d$ through transition functions: $\{f_t : \mathbb{R}^p \times \mathbb{R}^d \rightarrow \mathbb{R}^p\}_{t=1}^T$, $s_t = f_t(s_{t-1}; \theta)$ for T time steps starting from an initial state s_0 . At each time step $t \in \{1, \dots, T\}$, the state s_t incurs a loss $L_t^s(s_t)$. As the loss L_t^s depends on t applications of θ , we make this dependence more explicit with a loss function $L_t : \mathbb{R}^{dt} \rightarrow \mathbb{R}$ and $L_t([\theta]_{\times t}) := L_t^s(s_t)$.⁴ We aim to minimize the average loss over all T time steps unrolled under the same θ , $\min_{\theta} L([\theta]_{\times T})$, where

$$L(\theta_1, \dots, \theta_T) := \frac{1}{T} \sum_{t=1}^T L_t(\theta_1, \dots, \theta_t). \quad (1)$$

Although the loss is computed as an average over all steps, it can also encompass scenarios where we consider only a final loss at step T by expressing the final loss as a telescoping sum of loss differences [Beatson and Adams, 2019].

²Concurrent with our work, Vicol et al. [2023] independently propose a similar algorithm with different analyses.

³<https://github.com/OscarcLi/Noise-Reuse-Evolution-Strategies>

⁴We use the notation $[\theta]_{\times a}$, $a \in \mathbb{Z}_{\geq 0}$ to denote a copies of θ , for example: $L_t([\theta]_{\times a}, [\theta']_{\times t-a}) := L_t(\underbrace{\theta, \dots, \theta}_{a \text{ times}}, \underbrace{\theta', \dots, \theta'}_{(t-a) \text{ times}})$.

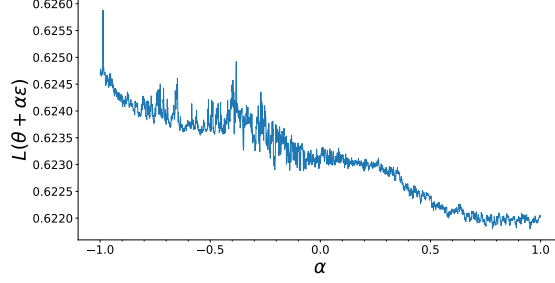


Figure 1: The chaotic loss surface in the learned optimizer task (Sec. 6.2) along a random ϵ direction. Due to high degrees of sharpness and the existence of many local minima, gradients of this loss surface are not informative; merely following the gradients through steepest descent is ineffective in minimizing the loss.

Automatic Differentiation. Automatic differentiation (AD) methods obtain gradient estimates by defining the gradients for each elementary function and composing them together through successive applications of the chain rule. Despite the existence of a large number of AD techniques to estimate gradients in UCGs, there exist scenarios where using AD methods are undesirable: **1) Chaotic loss surfaces:** With long unrolled computation graphs, the induced loss surface may have high degrees of sharpness (sharpness definition by Cohen et al. (2021)) (see Figure 1) or ill-conditioning. Naively following the true gradient may either **a)** fail to converge under the normal range of learning rates (because of the conflicting directions of gradients at close-by parameters) or **b)** converge to highly suboptimal solutions using a tuned, yet much smaller learning rate. **2) Inability to handle black-box computation dynamics or discontinuous losses:** As AD methods require defining a Jacobian-vector product (forward-mode differentiation) or a vector-Jacobian product (reverse-mode) for every elementary operation in the computation graph, AD methods cannot be applied when the unrolled computation graphs’ inner dynamics are inaccessible (e.g., model-free RL or complex physics simulator) or the loss objectives are piecewise constant (e.g. accuracy). Besides these foundational issues, AD methods can also suffer from issues such as large memory usage, online inapplicability, biasedness, and high variance (see details in Section 5).

Evolution Strategies. Due to these issues of AD in the above mentioned scenarios, a common alternative is to use Evolution Strategies (ES) to estimate gradients. Here an isotropic Gaussian distribution is convolved with the original loss function, resulting in an infinitely differentiable loss function with lower sharpness than before:

$$\theta \mapsto \mathbb{E}_{\epsilon \sim \mathcal{N}(\mathbf{0}, \sigma^2 I_{d \times d})} L([\theta + \epsilon]_{\times T}), \quad (2)$$

where $\sigma > 0$ is a hyperparameter. With the score function gradient estimator trick [Glynn, 1990], an unbiased estimator of (2) is given by $\frac{1}{\sigma^2} L([\theta + \epsilon]_{\times T}) \epsilon$. This estimator is zeroth-order since it only requires the loss function evaluation but not an explicit computation of its gradient, which allows for its effective use in cases when the gradients are noninformative (due to chaos) or not directly computable (black-box/discontinuous loss). To reduce the variance of this estimator, antithetic sampling is used and we call this finite-difference-style estimator FullES:

$$\text{FullES}(\theta) := \frac{1}{2\sigma^2} [L([\theta + \epsilon]_{\times T}) - L([\theta - \epsilon]_{\times T})] \epsilon. \quad (3)$$

Here the term Full highlights that this estimator can only produce a gradient estimate by averaging the antithetic particles’ losses (see Equation (1)) after a *full* unroll of T steps. This estimator can be massively parallelized (we denote the number of such *iid* estimators by N) [Salimans et al., 2017]; however, it is not online and might incur large latency between gradient updates when T is large.

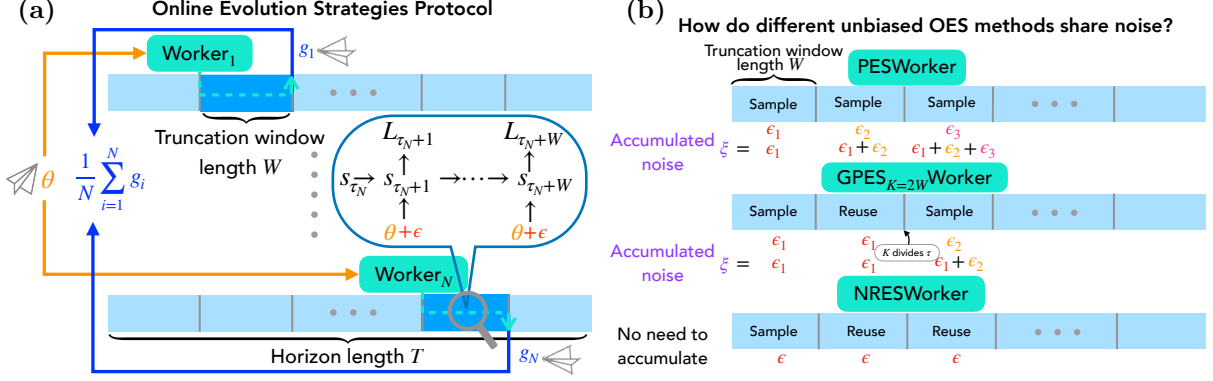


Figure 2: (a) Illustration of *step-unlocked* Online ES workers working independently at different truncation windows. Here a central server sends θ (whose gradient to be estimated) to each worker and receives the estimates over partial unrolls from each. The averaged gradient is then used in a first-order optimization algorithm (like Adam). (b) Comparison of the noise sharing mechanisms of PES, GPES $_K$, and NRES. Unlike PES (and GPES $_{K \neq T}$) which samples a new noise in every (some) truncation window and needs to accumulate the noise, NRES only samples noise once at the beginning of an episode, and reuses the noise for the full episode.

Truncated Evolution Strategies. To make FullES online, Metz et al. [2019] take inspiration from truncated backpropagation through time (TBPTT) and propose the algorithm TES (see an object-oriented python pseudocode in Algorithm 5 in the Appendix). Unlike the stateless estimator FullES, TES is stateful: Instead of starting from s_0 for every gradient estimate, the TESWorker picks up where it left off by starting the unrolling from a saved state s and drawing a new ϵ to compute the finite difference. In addition, unlike FullES, it only unrolls $2W$ steps (2 for antithetic) for every gradient estimate, thus allowing it to be used online and to incur lower latency between updates. Analytically, this gradient estimator can be expressed as:

$$\text{TES}(\theta) := \frac{1}{2\sigma^2 W} \sum_{i=1}^W [L_i([\theta]_{\times\tau}, [\theta + \epsilon]_{\times i}) - L_i([\theta]_{\times\tau}, [\theta - \epsilon]_{\times i})] \epsilon. \quad (4)$$

Here, besides the randomly sampled Gaussian random variable ϵ , the time step τ which TES starts from is also a random variable drawn from the uniform distribution $\tau \sim \text{Unif}\{0, W, \dots, T - W\}$ ⁵. For the rest of the paper, we will assume the time horizon T can be evenly divided into truncation windows of length W , i.e. $T \equiv 0 \pmod{W}$. It is worth noting that the prior work by Vicol et al. [2021] which also analyzes online ES estimators does not take the view that the time step τ an OES estimator starts from is a random variable; as such their analyses do not fully reflect the “online” nature captured in our work.

When multiple TESWorkers are used in parallel, different workers will be independently working at different time steps τ_i sampled from the same distribution $\text{Unif}\{0, W, \dots, T - W\}$ (which we call *step-unlocked* workers) (see Figure 2(a)). To make this happen, we need a preparation step to make the workers step-unlocked. We provide the pseudocode for this step and for general online ES learning in Algorithm 3 and Algorithm 4 in Appendix B.1.

Unfortunately, TES is biased relative to the gradient of (2): Notice in (4) that only the θ ’s inside the current length- W truncation window receive antithetic perturbations, thus ignoring the impact of the earlier applications of θ up to time step τ . Due to this bias, optimization using TES typically doesn’t converge to optimal solutions.

⁵For the rest of the paper, the random variable τ will always be sampled from this distribution.

Persistent Evolution Strategies. To resolve the bias of TES, [Vicol et al. \(2021\)](#) take into account the fact that TES samples a new noise vector to use within every truncation window and modifies the smoothing objective into:

$$\theta \mapsto \mathbb{E}_{\{\epsilon_i\}} L([\theta + \epsilon_1]_{\times W}, \dots, [\theta + \epsilon_{T/W}]_{\times W}), \quad (5)$$

with $\epsilon_i|_{i=1}^{T/W} \stackrel{\text{iid}}{\sim} \mathcal{N}(\mathbf{0}, \sigma^2 I_{d \times d})$. Under this new objective, [Vicol et al. \[2021\]](#) show that an unbiased gradient estimator is given by

$$\begin{aligned} \text{PES}(\theta) := \frac{1}{2\sigma^2 W} \sum_{j=1}^W & \left[L_{\tau+j}([\theta + \epsilon_1]_{\times W}, \dots, [\theta + \epsilon_{(\tau/W)+1}]_{\times j}) \right. \\ & \left. - L_{\tau+j}([\theta - \epsilon_1]_{\times W}, \dots, [\theta - \epsilon_{(\tau/W)+1}]_{\times j}) \right] \left(\sum_{i=1}^{\tau/W} \epsilon_i + \epsilon_{\tau/W+1} \right), \end{aligned} \quad (6)$$

with randomness in both $\{\epsilon_i\}$ and τ . Pseudocode is given in Algorithm 1. To eliminate the bias of TES, instead of multiplying the finite difference with only the current epsilon $\epsilon_{\tau/W+1}$, PES multiplies it with the cumulative sum of all the different *iid* noise sampled so far (`self.ξ` in `PESWorker`).

Algorithm 1 Persistent Evolution Strategies (PES)

class `PESWorker`(`OESWorker`):

def `__init__`(`self`, `W`):

`self.τ` = 0; `self.s+` = `s0`; `self.s-` = `s0`

`self.W` = `W`, `self.ξ` = `0` ∈ \mathbb{R}^d

def `gradient_estimate`(`self`, `θ`):

$\epsilon \sim \mathcal{N}(\mathbf{0}, \sigma^2 I_{d \times d})$

 # this is $\epsilon_{(\tau/W)+1}$

`self.ξ` += ϵ

 # now `self.ξ` = $\sum_{i=1}^{\tau/W} \epsilon_i + \epsilon_{\tau/W+1}$

$(s^+, s^-) = (\text{self}.s^+, \text{self}.s^-)$

`Lsum+` = 0; `Lsum-` = 0

for `i` **in** `range`(1, `self.W`+1):

$s^+ = f_{\text{self.}\tau+i}(s^+, \theta + \epsilon)$; $s^- = f_{\text{self.}\tau+i}(s^-, \theta - \epsilon)$

`Lsum+` += $L_{\tau+i}^s(s^+)$; `Lsum-` += $L_{\tau+i}^s(s^-)$

$g = (L_{\text{sum}}^+ - L_{\text{sum}}^-) / (2\sigma^2 \cdot \text{self.W}) \cdot \text{self.ξ}$

`self.s+` = s^+ ; `self.s-` = s^-

`self.τ` = `τ` + `W`

if `self.τ` ≥ `T`:

 # reset at the end of an episode

`self.τ` = 0; `self.s+` = `s0`; `self.s-` = `s0`; `self.ξ` = `0`

return `g`

Hysteresis. When online gradient estimators are used for training, they often suffer from hysteresis, or history dependence, as a result of the parameters θ at which the function is being evaluated changing between unrolls. That is, the parameter value θ_0 that a worker uses in the current truncation window will be inconsistent with the parameter value θ_{-1} that was used in the previous window. Algorithms which suffer from hysteresis include TES, PES, and AD forward mode methods like UORO [[Tallec and Ollivier, 2017a](#)] and DODGE [[Silver et al., 2021](#)]. This effect is often neglected, under an assumption that θ is updated slowly. To the best of our knowledge, [[Massé and Ollivier, 2020](#)] is the only work that has analyzed the convergence of an online gradient estimator under hysteresis. In the following theoretical analysis, we assume all online gradient estimates are computed without hysteresis in order to isolate the problem. In Section 6, we show experimentally that even under the impact of hysteresis, our proposed online estimator NRES can outperform non-online methods (e.g., FULLES) which don't suffer from hysteresis.

3 Generalizing PES

As we have seen in Section 2, a similarity between TES and PES is that they both sample a new noise vector ϵ to use for every new truncation window to produce a gradient estimate. Here we note that the *frequency of noise-sharing* (new noise every truncation window of size W) is fixed to the *frequency of gradient estimates* (a gradient estimate every truncation window of size W). However, the former is a choice of the smoothing objective ((2) and (5)), while the latter is often a choice of hardware/optimization iteration speed. We break this coupling in this section by introducing a general class of gradient estimators that encompass PES. We then analyze these estimators' variance to identify the one with the least variance.

Generalized Persistent Evolution Strategies (GPES). For a given fixed truncation window size W , we consider all *noise-sharing periods* K that are multiples of W , $K = cW$ for $c \in \mathbb{Z}^+$, $c \leq T/W$. K being a multiple of W ensures that within each truncation window, only a single ϵ is used. When $K = W$, we recover the PES algorithm. However, when K is larger than W , the same noise will be used across adjacent truncation windows (Figure 2(b)). With a new noise sampled every K unroll steps, we define the K -smoothed loss objective as the function⁶:

$$\theta \mapsto \mathbb{E}_{\{\epsilon_i\}} L([\theta + \epsilon_1]_{\times K}, \dots, [\theta + \epsilon_{\lceil T/K \rceil}]_{\times r(T,K)}), \quad (7)$$

where $r : (\mathbb{Z}^+)^2 \rightarrow \mathbb{Z}^+$ is the modified remainder function such that $r(x, y)$ is the unique integer $n \in [1, y]$ where $x = qy + n$ for some integer q . This extra notation allows for the possibility that T is not divisible by K and the last noise $\epsilon_{\lceil T/K \rceil}$ is used over only $r(T, K) < K$ steps.

We now give the analytic form for gradient estimation of the resulting smoothed loss.⁷

Lemma 1. *An unbiased gradient estimator for the K -smoothed loss is given by*

$$\text{GPES}_{K=cW}(\theta) := \frac{1}{2\sigma^2 W} \sum_{j=1}^W \left[L_{\tau+j}([\theta + \epsilon_1]_{\times K}, \dots, [\theta + \epsilon_{\lceil \tau/K \rceil + 1}]_{\times r(\tau+j, K)}) \right. \\ \left. - L_{\tau+j}([\theta + \epsilon_1]_{\times K}, \dots, [\theta + \epsilon_{\lceil \tau/K \rceil + 1}]_{\times r(\tau+j, K)}) \right] \cdot \left(\sum_{i=1}^{\lceil \tau/K \rceil + 1} \epsilon_i \right),$$

with randomness in τ and $\{\epsilon_i\}_{i=1}^{\lceil T/K \rceil}$.

Here, for the truncation window starting at step τ , the noise $\epsilon_{\lceil \tau/K \rceil + 1}$ is used to unroll the system. If τ is not divisible by K , then this noise has already been sampled at the truncation window beginning at step $\lceil \tau/K \rceil \cdot K$. Therefore, to know what noise to apply at this truncation window, we need to remember the last used ϵ and update it when τ becomes divisible by K . With this understanding, we can write down the algorithm for the GPES_K gradient estimator in Algorithm 2. Note that $\text{GPES}_{K=W}$ is the same as the PES algorithm.

Variance Characterization of GPES. With this generalized class of gradient estimators GPES_K , one might wonder how to choose the value of K . Since each estimator is unbiased with respect to its own smoothed objective's true gradient (first moment), we compare the second moment (variance) of these estimators as a function of K . To do this analytically, we make some simplifying assumptions:

⁶ $\lceil x \rceil$ is smallest integer $\geq x$; $\lfloor x \rfloor$ is the largest integer $\leq x$.

⁷Proofs for all the Lemmas and Theorems are in Appendix C.

Algorithm 2 Generalized Persistent Evolution Strategies (GPES)

class GPESWorker(OESWorker):

```
def __init__(self, W, K):
    self.τ = 0; self.s+ = s0; self.s- = s0
    self.W = W; self.K = K; self.ξ = 0 ∈ ℝd

def gradient_estimate(self, θ):
    # only sample a new ε when condition is satisfied
    if self.τ % self.K == 0:
        εnew ~ N(0, σ2Id×d)
        # keep track of εnew to use for the next K steps
        self.ε = εnew
        self.ξ += εnew
    # after the if statement above, self.ε is now ε[self.τ/K]+1
    # and self.ξ is now ∑i=1[τ/K]+1 εi
    (s+, s-) = (self.s+, self.s-)
    Lsum+ = 0; Lsum- = 0
    for i in range(1, self.W+1):
        s+ = fself.τ+i(s+, θ + self.ε)
        s- = fself.τ+i(s-, θ - self.ε)
        Lsum+ += Lself.τ+is(s+); Lsum- += Lself.τ+is(s-)
    g = (Lsum+ - Lsum-) / (2σ2 · self.W) · self.ξ
    self.s+ = s+; self.s- = s-
    self.τ = self.τ + W
    if self.τ ≥ T: # reset at the end of an episode
        self.τ = 0; self.s+ = s0; self.s- = s0; self.ξ = 0
    return g
```

Assumption 2. For a given $\theta \in \mathbb{R}^d$ and $t \in [T]$, there exists a set of vectors $\{g_i^t \in \mathbb{R}^d\}_{i=1}^t$, such that for any $\{v_i \in \mathbb{R}^d\}_{i=1}^t$, the following equality holds:

$$L_t(\theta + v_1, \theta + v_2, \dots, \theta + v_t) - L_t(\theta - v_1, \theta - v_2, \dots, \theta - v_t) = 2 \sum_{i=1}^t (v_i)^\top (g_i^t) \quad (8)$$

Remark 3. This assumption is more general than the quadratic L_t assumption made in [Vicol et al., 2021]. Here one can roughly understand g_i^t as time step t 's smoothed loss's partial derivative with respect to the i -th application of θ . For notational convenience, we let $g^t := \sum_{i=1}^t g_i^t$ (roughly the total derivative of smoothed step- t loss with respect to θ) and $g_{K,j}^t := \sum_{i=K \cdot (j-1)+1}^{\min\{t, K \cdot j\}} g_i^t$ for $j \in \{1, \dots, \lceil t/K \rceil\}$ (the sum of partial derivatives of smoothed step- t loss with respect to all θ 's in the j -th noise-sharing window of size K (the last window might be shorter)).

With this assumption in place, we first consider the case when $W = 1$ and $K = cW = c$. In this case, the GPES _{K} estimator can be simplified into the following form:

Lemma 4. Under Assumption 2, when $W = 1$, $\text{GPES}_{K=c}(\theta) = \frac{1}{\sigma^2} \sum_{j=1}^{\lceil \tau/c \rceil + 1} \left(\sum_{i=1}^{\lceil \tau/c \rceil + 1} \epsilon_i \right) \epsilon_j^\top g_{c,j}^{\tau+1}$, where the randomness lies in τ and $\{\epsilon_i\}$.

With this simplified form, we can now characterize the variance of the estimator $\text{GPES}_{K=c}(\theta)$. Since it's a random vector, we analytically derive its total variance (trace of covariance matrix) $\text{tr}(\text{Cov}[\text{GPES}_{K=c}(\theta)])$.

Theorem 5. When $W = 1$ and under Assumption 2, the total variance of $\text{GPES}_{K=c}(\theta)$ for integer $c \in [1, T]$ is

$$\text{tr}(\text{Cov}[\text{GPES}_{K=c}(\theta)]) = \underbrace{\frac{(d+2)}{T} \sum_{t=1}^T (\|g^t\|_2^2)}_{\textcircled{1}} - \underbrace{\left\| \frac{1}{T} \sum_{t=1}^T g^t \right\|_2^2}_{\textcircled{2}} + \underbrace{\frac{1}{T} \sum_{t=1}^T \left(\frac{d}{2} \sum_{j=1, j' \neq j}^{\lceil t/c \rceil} \|g_{c,j}^t - g_{c,j'}^t\|_2^2 \right)}_{\textcircled{3}}. \quad (9)$$

To understand how the value of $K = c$ changes the total variation, we notice that only the nonnegative third term $\textcircled{3}$ in (9) depends on it. This term measures the pairwise squared distance between non-overlapping partial sums $g_{c,j}^t$ for each j . When $c = T$, for every $t \in [1, T]$, there is only a single such partial sum as $\lceil t/c \rceil = 1$. In this case, this third term reduces to its smallest value of 0. Thus:

Corollary 6. Under Assumption 2, when $W = 1$, the gradient estimator $\text{GPES}_{K=T}(\theta)$ has the smallest total variance among all $\{\text{GPES}_K : K \in [T]\}$ estimators.

Experimental Verification of Corollary 6. We empirically verify Corollary 6 on a meta-training learned optimizer task ($T = 1000$; see additional details in Section 6.2). Here we save a trajectory of θ_i learned by PES (i denotes training iteration) and compute the total variance of the estimated gradients (without hysteresis) by GPES with different values of K in Figure 3 ($W = 1$). In agreement with theory, $K = T$ has the lowest variance.

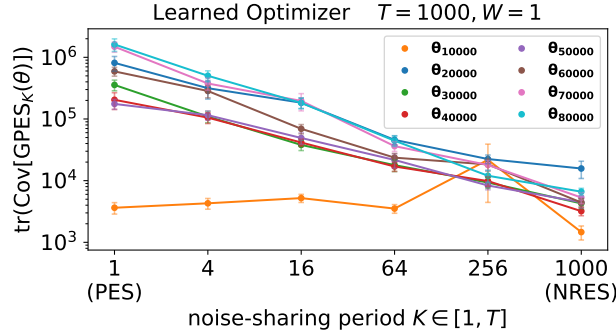


Figure 3: $\text{tr}(\text{Cov}[\text{GPES}_K(\theta_i)])$ vs. noise-sharing period K for different θ_i 's from the learned trajectory of PES. $\text{GPES}_{K=T}$ (NRES) has the lowest total variance among estimators of its class (including PES).

4 Noise Reuse Evolution Strategies

As variance reduction is desirable in stochastic optimization [Wang et al., 2013], by Corollary 6, the gradient estimator $\text{GPES}_{K=T}$ is particularly attractive and *can serve as a variance-reduced replacement for PES*. When $K = T$, we see in Algorithm 2 that for this worker we only need to sample a single ϵ once at the beginning of an episode (When $\tau = 0$) and reuse the same noise for the entirety of that episode before it resets. This reduces the need to keep track of the cumulative applied noise (ξ), making the algorithm simpler and more memory efficient than PES (Figure 2). Due to its noise-reuse property, we call this gradient estimator $\text{GPES}_{K=T}$ the *Noise Reuse Evolution Strategies* (NRES). See Appendix B.3 for the complete algorithm pseudocode.

Despite Theorem 5 assuming $W = 1$, one can relax this assumption to any W that divides the horizon length T . By defining a mega UCG whose single transition step is equivalent to W steps in the original UCG, we can then apply Corollary 6 to this mega UCG and arrive at the following result.

Corollary 7. *Under Assumption 2, when W divides T , the NRES gradient estimator has the smallest total variance among all $\text{GPES}_{K=cW}$ estimators $c \in \mathbb{Z} \cap [1, T/W]$.*

NRES as a replacement for FullES. We note that by sharing the same noise over the entire horizon, the smoothing objective of NRES becomes the same as that of FullES. As a result, we can think of NRES as the online counterpart to the offline algorithm FullES. In many places where FullES is used, NRES can act as a drop-in replacement to reduce gradient estimate latency. A single FullES worker runs $2T$ unroll steps for each gradient estimate, while a single NRES runs only $2W$. Motivated by this, we compare the variance of the average of T/W independent NRES gradient estimates with the variance of 1 FullES estimate:

Theorem 8. *Under Assumption 2, for any W that divides T , if*

$$\sum_{k=1}^{T/W} \left\| \sum_{t=W \cdot (k-1)+1}^{W \cdot k} g^t \right\|_2^2 \leq \frac{d+1}{d+2} \left\| \sum_{j=1}^{T/W} \sum_{t=W \cdot (j-1)+1}^{W \cdot j} g^t \right\|_2^2, \quad (10)$$

then

$$\text{tr}(\text{Cov}(\frac{1}{T/W} \sum_{i=1}^{T/W} \text{NRES}_i(\theta))) \leq \text{tr}(\text{Cov}(\text{FullES}(\theta))), \quad (11)$$

where $\text{NRES}_i(\theta)$ are iid NRES estimators.

Here inequality (10) relates the sum of squared 2-norm of vectors $\sum_{t=W \cdot (k-1)+1}^{W \cdot k} g^t$ with the squared 2-norm of their sum. When these vectors are pointing in similar directions, this inequality would hold. Semantically speaking, each term $\sum_{t=W \cdot (k-1)+1}^{W \cdot k} g^t$ can be understood as the total derivative of the sum of smoothed losses within the k -th truncation window with respect to θ . Thus we see that inequality (10) is satisfied when, roughly speaking, different truncation windows' gradient contributions are pointing in similar directions. This is often the case for real-world applications because if we can decrease the losses inside a given truncation window by changing the parameter θ , we will likely also decrease other truncation windows' losses. At a high-level, Theorem 8 tells us that NRES is a more suitable gradient estimator than FullES for many practical unrolled computation graphs – with the same amount of computation budget, NRES's gradient estimates not only has lower variance than FullES but also have lower computation latency (one needs to wait only $O(W)$ for an NRES update instead of $O(T)$ for an FullES update).

Empirical Verification of Theorem 8. We empirically verify Theorem 8 in Table 1 using the same set up of the meta-training learned optimizer task used in Figure 3. Here we compare running $T/W = 1000/1 = 1000$ iid NRES estimators in parallel versus running 1 FullES gradient estimator (same total amount of compute) in terms of their total variance. We see that NRES estimators has a significantly lower total variance than FullES while also allowing $T/W = 1000$ times wall-clock speed up due to the parallelization.

Table 1: Comparing the total variance (with 95% confidence interval) of NRES and FullES estimators ($T = 1000, W = 1$) under the same computation budget at different θ_i checkpoints from the learned optimizer trajectory by PES. NRES estimators consistently has lower total covariance.

iteration i of θ_i	$\text{tr}(\text{Cov}(\frac{1}{T/W} \sum_{i=1}^{T/W} \text{NRES}_i(\theta)))$	$\text{tr}(\text{Cov}(\text{FullES}(\theta)))$
10000	1.47 \pm 0.38	864.34 \pm 385.01
20000	15.74 \pm 4.90	513.50 \pm 74.71
30000	4.28 \pm 0.78	201.38 \pm 30.18
40000	3.20 \pm 0.50	684.85 \pm 86.90
50000	4.47 \pm 0.88	181.06 \pm 24.97
60000	4.42 \pm 0.68	288.61 \pm 46.77
70000	5.33 \pm 1.08	448.30 \pm 62.44
80000	6.62 \pm 0.89	154.86 \pm 28.21

5 Related Work

In this section we further position NRES relative to existing gradient estimation methods, and describe the baselines we compare to in our experiments.

Reverse Mode Differentiation (RMD). When the loss function and transition functions in UCG is differentiable, the default method for computing gradients is backpropagation through time (BPTT). However, BPTT has difficulties when applied to UCGs: **1) *memory issues*:** the default BPTT implementations [e.g., Abadi, 2016, Paszke et al., 2019] store all activations of the graph in memory, making memory usage scale linearly with the length of the unrolled graph. There are works that improve the memory dependency of BPTT; however, they either require customized framework implementation [Chen et al., 2016, Tallec and Ollivier, 2017b] or specially-designed reversible computation dynamics [Maclaurin et al., 2015, Gomez et al., 2017]. **2) *offline*:** each gradient estimate using BPTT requires full forward and backward computation through the UCG, which is computationally expensive and incurs large latency between successive parameter updates. To alleviate the memory issue and allow online updates, a popular alternative is truncated backpropagation through time (TBPTT) which estimates the gradient within short truncation windows. However, this blocks the gradient flow to the parameters applied before the current window, making the gradient estimate biased and unable to capture long-term dependencies [Wu et al., 2018]. In contrast, NRES is memory efficient, online, and doesn’t suffer from bias, while also being able to handle chaotic loss surfaces.

Forward Mode Differentiation (FMD). An alternative to RMD in automatic differentiation is FMD, which computes gradient estimates through Jacobian-vector products alongside the actual forward computation. Among FMD methods, real-time recurrent learning (RTRL) [Williams and Zipser, 1989] requires a computation cost that scales with the dimension of the learnable parameter, making it intractable for large problems. To alleviate the computation cost, stochastic approximations of RTRL have been proposed: DODGE [Silver et al., 2021] computes directional gradient along a certain direction; UORO [Tallec and Ollivier, 2017a] unbiasedly approximates the Jacobian with a rank-1 matrix; KF – RTRL [Mujika et al., 2018] and OK [Benzing et al., 2019] uses Kronecker product decomposition to improve the gradient estimate’s variance, but are specifically for RNNs. In Section 6, we compare against DODGE (with standard Gaussian random directions) and UORO and demonstrate NRES’s advantage over these two online and memory-efficient methods when the loss surface is chaotic.

Zeroth-Order Gradient Estimators. In this work we focus on methods that can estimate continuous parameters’ gradients and can be plugged directly into first-order optimizers, unlike zeroth-order optimization methods such as Bayesian Optimization [Frazier, 2018], random search [Bergstra and Bengio, 2012], or Trust Region methods [Maggiar et al., 2018, Liu et al., 2019]. We also don’t compare against policy gradient methods [Sutton et al., 1999], as these approaches assume internal stochasticity of the unrolling dynamics which may not hold for deterministic policy learning [e.g., Todorov et al., 2012]. Within the space of evolution strategies (ES) methods, many works have focused on improving the vanilla ES method’s variance by changing the type of perturbation distribution [Choromanski et al., 2018, Maheswaranathan et al., 2019, Agapie, 2021, Gao and Sener, 2022], additionally considering covariance structure [Hansen, 2016], and using control variates [Tang et al., 2020]. However, these works do not consider the unrolled structure of the UCGs and are offline methods. In contrast, we reduce the variance by incorporating this additional information through online estimation and additionally outperform existing the online method PES through noise-reuse. As the aforementioned variance reduction methods work orthogonally to NRES, it is conceivable that these techniques can be used in conjunction with NRES to further reduce the variance.

6 Experiments

NRES is particularly suitable for two common scenarios: 1) when the loss surface has high sharpness and exhibits chaotic behavior; 2) when differentiation through the loss/dynamics is not possible. In this section, we focus on three applications exhibiting these properties: a) learning Lorenz system’s parameters from data (chaotic), b) meta-training learned optimizers (chaotic), and c) reinforcement learning (nondifferentiable), and show NRES outperforms existing AD methods (described in Section 5 RMD and FMD) and ES methods for these applications. For each application, we use the same σ value for all ES methods after tuning it first on FullES.

6.1 Learning dynamical system parameters

In this application, we consider learning the parameters of a Lorenz system, a canonical chaotic dynamical system. Here the state $s_t = (x_t, y_t, z_t) \in \mathbb{R}^3$ is unrolled with two learnable parameters a, r ⁸ with the discretized transitions:

$$\begin{aligned}x_{t+1} &= x_t + a(y_t - x_t)dt \\y_{t+1} &= y_t + [x_t \cdot (r - z_t) - y_t]dt \\z_{t+1} &= z_t + [x_t \cdot y_t - 8/3 \cdot z_t]dt\end{aligned}\tag{12}$$

with $dt = 0.005$. Due to the positive constraint on $a > 0$ and $r > 0$, we parameterize them as $\theta = (\ln(a), \ln(r)) \in \mathbb{R}^2$, and exponentiate the values during each application. We assume we observe the initial state of the canonical Lorenz system $s_0 = (x_0, y_0, z_0) = (1.2, 1.3, 1.6)$ and then only the ground truth z_t^{gt} for $t \in \{1, \dots, T = 2000\}$ unrolled by the canonical Lorenz system’s parameters $(a^{\text{gt}}, r^{\text{gt}}) = (10, 28)$. For each step t , we measure the squared loss $L_t^s(s_t) := (z_t - z_t^{\text{gt}})^2$. Our goal is to recover the ground truth parameters by optimizing the average loss over all time steps using vanilla SGD. We first visualize the training loss surface around the ground truth solution in Figure 4 (a) and notice that the training loss surface is highly chaotic.

To illustrate the superior variance properties of NRES over other estimators in the GPES_K class, we plot in Figure 4 (b) the optimization trajectory of θ using gradient estimators GPES_K with different values of K using

⁸We don’t learn a third parameter, fixed at $8/3$, so that we can easily visualize a 2-d loss surface.

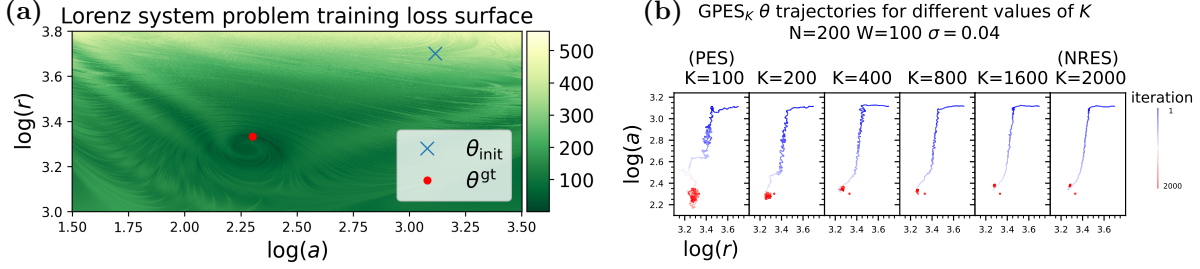


Figure 4: (a) The training loss surface in the learning Lorenz System parameters problem 6.1 is highly chaotic. (b) The optimization trajectory of different GPES_K gradient estimators (starting from the same initialization) under the same SGD learning rate of 10^{-5} .

the same number of workers $N = 200$, same truncation window size $W = 100$, and the same SGD learning rate of 10^{-5} . Here we see that among all the GPES_K trajectories considered, NRES’s trajectory exhibits the least random oscillation: in addition to stably converging after 2000 SGD updates, the convergence trajectory is also the smoothest.

From this result, we observe that because of the higher variance of PES than NRES, PES needs a smaller learning rate than NRES to achieve a stable (yet possibly slower) convergence. Thus we take extra care in tuning each method’s learning rate and additionally allow PES to have a decay schedule. We plot the convergence speed (averaged over 5 random seeds) of different gradient estimators in wall-clock time using the same hardware in Figure 5. Here we measure the test loss instead of the training loss by sampling the random initial state $s_0 \sim \mathcal{N}((1.2, 1.3, 1.6), 0.01 I_{3 \times 3})$. This is because the highly chaotic training loss surface makes all gradient estimation methods’ training loss progressions have significant fluctuations, thus difficult to make meaningful visual comparisons of. In addition, the test loss is a better indicator of predictive generalization to novel initial state conditions.

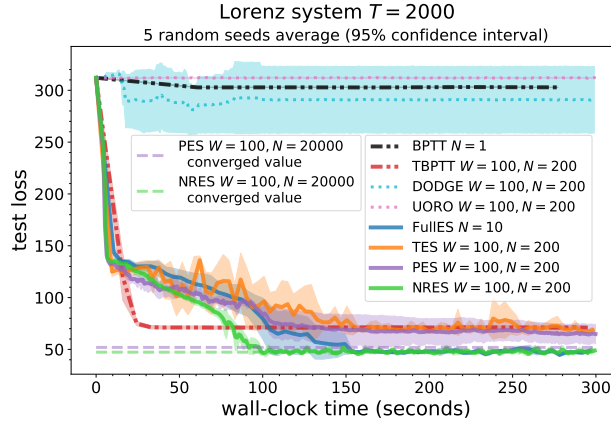


Figure 5: We compare the test loss convergence of different gradient estimators in wall-clock time using the same hardware on the Lorenz system parameter learning problem. NRES converges to the lowest value fastest among all the methods.

In terms of the result, we first notice that the AD methods that unbiasedly estimate the nonsmoothed loss surface’s gradient (BPTT, DODGE, UORO) all fail to make much progress due to the chaotic gradients. Among the rest of the methods, NRES outperforms 1) TBPTT and TES, because, unlike these two methods,

NRES is unbiased and can better capture the long-term dependency; **2)** outperforms FullES⁹, because every NRES update only takes $O(W)$ time instead of FullES’s $O(T)$ time when both are implemented with parallelization, allowing NRES to afford many more updates in the same amount of wall-clock time than FullES; outperforms **3)** PES because of NRES’s improved variance. Additionally, we plot the asymptotically converged test loss value when we train with a significantly larger number of particles ($N = 20000$) for PES and NRES. We see that by only using $N = 200$ particles, NRES can already stably converge around this asymptotic limit, while PES is still far from reaching its asymptotic limit within our experiment time.

6.2 Meta-training learned optimizers

In this application, the meta-parameters θ of a learned optimizer control the gradient-based updates of an inner-problem’s parameters. The inner state s_t holds the inner problem’s parameters and momentum statistics; the transition function f_t **1)** computes the training loss gradient of the inner-model parameters over a random training batch, **2)** applies the learned optimizer with parameters θ to generate an inner-parameter update vector given this gradient and s_t , **3)** and add this update vector to the current model parameters to form the next state s_{t+1} . The meta-loss L_t^s is evaluated over the updated model parameters using a sampled batch from a held-out validation set to encourage generalization to unseen data.

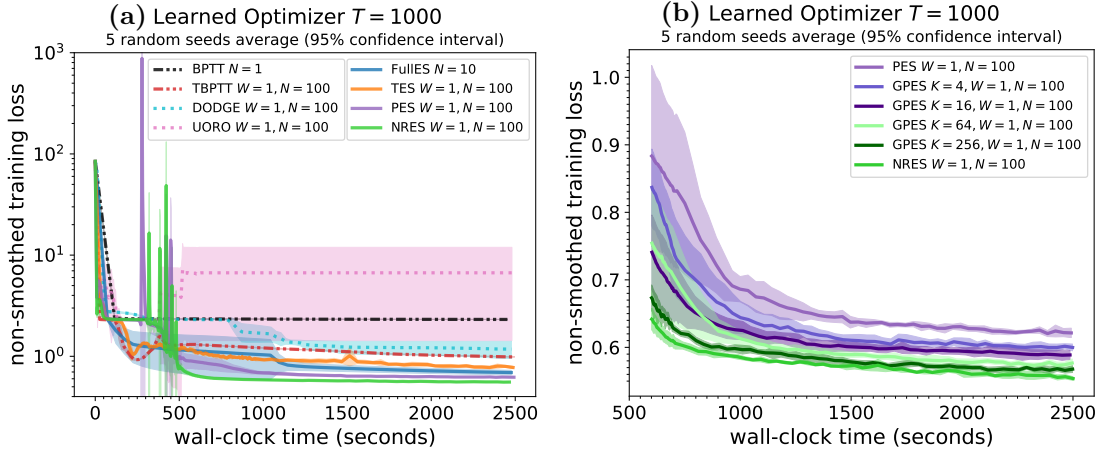


Figure 6: (a) We compare the learned optimizer training loss convergence using different gradient estimators in wall-clock time. NRES reaches the lowest loss fastest. (b) We compare NRES’s convergence with other gradient estimators in the GPES $_K$ class on the learned optimizer task. NRES converges fastest due to its reduced variance. (c) We compare different ES methods’ sample complexity in solving the Mujoco Swimmer-v4 task. NRES solves the task using the least number of environment steps when averaged over 5 random seeds.

We consider a learned optimizer setting where the inner problem is training a 3-layer 32-width gelu-activated MLP over the Fashion MNIST dataset for $T = 1000$ steps, and we use the meta-optimizer architecture given in [Metz et al., 2019] ($d = 1762$). Tasks of this scale is used in the training task distribution of state of the art learned optimizer VeLO [Metz et al., 2022a]. For this specific problem, the entire UCG can fit on a single GPU card to allow for the use of BPTT without memory issues. We fix the sequence of data batches for inner-training and meta-loss evaluation to isolate the randomness to only the stochastic gradient estimator. The loss surface for this problem has high sharpness and many local nonoptimal minima as shown in Figure 1. We meta-train with Adam using gradients generated by different AD and ES methods. For each method,

⁹If we compare the mean time it takes NRES and FullES to reach the asymptotic test loss in Figure 5, NRES reduces more than 30% of the time used by FullES.

we run it using the same amount of hardware resources and tune its meta learning rate (used for Adam) (details in Appendix D.1.2).

We plot the nonsmoothed training loss progress of different methods in wall-clock time (averaged over 5 random seeds) in Figure 6. Here we notice that both BPTT and UORO fail to improve over random guessing ($\ln(10) \approx 2.3$), because the learning rate must be tuned very small to prevent exploding gradients from causing training to diverge. For the rest of the estimators, we see that NRES reaches the lowest loss value fastest¹⁰. To further understand the performance difference among the top three methods (NRES, PES, FullES), we show in Figure 8 in Appendix D.2 that PES and FullES would require 5 and 10 times longer than NRES to reach a loss NRES reaches relatively early on during its training. In addition, we also situate NRES’s performance within our proposed class of GPES_K estimators with different values of K in Figure 6(b). Here for all the GPES methods (including PES and NRES), we use the same tuned Adam learning rate of 3×10^{-4} . We see that NRES converge to the lowest value among all GPES_K estimators due to its reduced variance.

6.3 Reinforcement Learning

It has been shown that ES is a scalable alternative to policy gradient and value function methods for solving reinforcement learning tasks [Salimans et al., 2017]. In this application, we learn a linear policy (following Mania et al. (2018)) using different ES methods for the Mujoco [Todorov et al., 2012] Swimmer-v4 task ($d = 16$) and Half Cheetah-v4 task ($d = 102$). We minimize the negative of the average reward over the horizon length of $T = 1000$, which is equivalent to maximizing the undiscounted total rewards. Unlike Salimans et al. (2017), Mania et al. (2018), and Vicol et al. (2021), we don’t use additional heuristic tricks like **1**) rank conversion of rewards, **2**) scaling by loss standard deviation, or **3**) state normalization. Instead, we aim to test the pure performance of different ES methods in terms of their sample complexity (total number of environment steps). We tune the SGD learning rate individually for each method. We plot the total rewards progression of different methods on both Mujoco tasks in Figure 7.

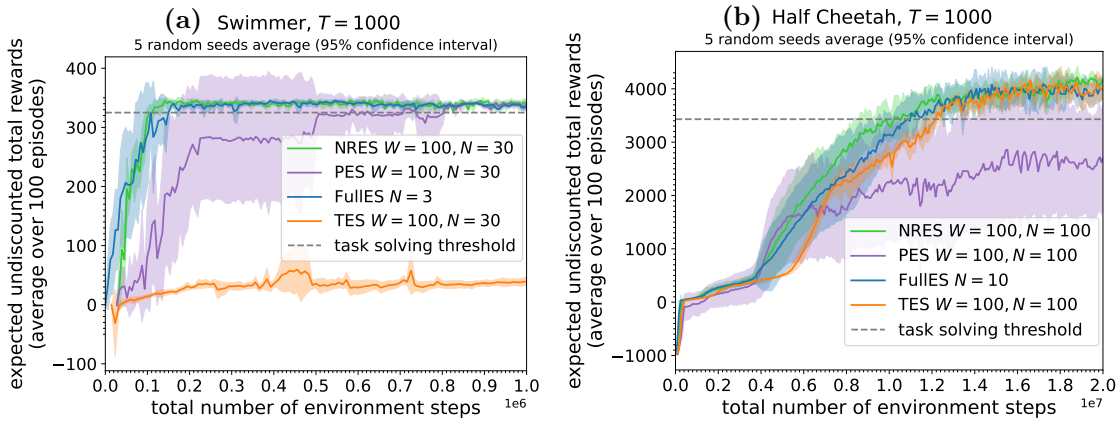


Figure 7: We compare different ES methods’ sample complexity in solving the Mujoco (a) Swimmer-v4 task and (b) Half Cheetah-v4 task. NRES solves the tasks using the least number of environment steps when averaged over 5 random seeds.

Here we discuss the advantage of NRES over other ES methods separately:

¹⁰For both PES and NRES, there is a short period of fluctuation in the loss before 500 seconds. We believe this is a property of this specific application but not problems of the methods since this phenomenon doesn’t occur in other applications.

- [TES] Unlike NRES, TES fails to solve the Swimmer-v4 task (target reward = 325) because its gradient estimates suffer from the short horizon bias, making it unable to capture long term dependencies necessary to solve the task.
- [PES] Compared to PES, we see that NRES can solve both tasks using much fewer number of environment steps, again confirming our insight of NRES’s variance reduction benefit over PES.
- [FullES] From Figure 7 alone, one might wonder whether NRES can only improve over FullES by < 30%. However, we want to point out that the unit of measure on the horizontal axis is hiding the **significance** of the improvement of NRES over FullES – for both of the Mujoco tasks, we only measure the total number of environment steps used by each ES gradient estimation method but not the total wall-clock time it takes. This is because the official Mujoco task simulation¹¹ is CPU-based which does not provide true parallelization capabilities unless we use a distributed multi-machine infrastructure. To make our research easily reproducible on a single machine, we choose not to implement our method for a distributed infrastructure. However, if we were to use a truly parallel implementation¹², NRES’s *required wall-clock time to solve the Swimmer and Half Cheetah task would be < 10% of FullES’s required wall-clock time*. This can be directly inferred from Figure 7 because **1)** every gradient update of NRES takes $O(W)$ time (truncation window of size W) instead of $O(T)$ by FullES, making NRES takes around $W/T = 100/1000 = 10\%$ of the time that FullES takes to produce a gradient estimate; **2)** both NRES and FullES use roughly the same number of gradient updates to solve the each Mujoco task¹³.

7 Discussion, Limitations, and Future Work

In this work, we improve Online Evolution Strategies for unbiased gradient estimation in unrolled computation graphs by analyzing the best noise-sharing strategies. By generalizing an existing unbiased method, Persistent Evolution Strategies, to a broader class, we identify the best estimator with the smallest variance (both analytically and empirically) and name it Noise Reuse Evolution Strategies (NRES) due to its noise reuse property. We demonstrate the convergence benefits of NRES over other automatic differentiation and evolution strategies methods on a variety of applications.

As we have shown through multiple applications in Section 6, NRES can be an ideal choice of gradient estimator when the loss surface is chaotic or non-differentiable. However, just as any other useful tool in the modern machine learning toolbox, NRES should only be used in these most suited scenarios. Here, we additionally discuss limitations of NRES (which are often limitations shared by a class of methods NRES belongs to) and in what scenarios it might not be the first choice to use.

Limitations of NRES as an Evolution Strategies method. Here we discuss the limitations of NRES as an ES method (both limitations below are common to all ES methods).

- **[Dependence on d]** As all the Evolution Strategies methods only have access to zeroth-order information, their variance has a linear dependence on the parameter dimension d (see term ① in Theorem 5). As a result, the most ideal use cases of ES methods (including NRES) are when the parameter dimension d is lower than 100,000. As we have seen in Section 6, many interesting applications would have parameter dimensions in this range. However, even in cases when d is larger than this range, if the loss

¹¹OpenAI gymnasium. <https://gymnasium.farama.org/>

¹²See [Salimans et al., 2017] for an example implementation. <https://github.com/openai/evolution-strategies-starter>

¹³This is because **a)** NRES and FullES use roughly the same total number of environment steps to solve the task, and **b)** every NRES and FullES gradient update takes the same number of environment steps (e.g., for the Swimmer-v4 task, NRES takes $2 \cdot N_{\text{NRES}} \cdot W = 2 \cdot 30 \cdot 100 = 6000$ steps while FullES also takes $2 \cdot N_{\text{FullES}} \cdot T = 2 \cdot 3 \cdot 1000 = 6000$ steps).

surface is non-differentiable or chaotic, one might still need to use NRES because AD methods might either be unable to compute the gradient or give noninformative gradients for effective optimization. On the other hand, AD methods (specifically Reverse Mode Differentiation methods (BPTT and TBPTT)) should be the first choice when the parameter dimension is large and the loss surface is differentiable and well-behaved, because their variance doesn't suffer from a linear dependence on d .

- **[Dependence on σ]** The variance σ of the smoothing isotropic Gaussian distribution for ϵ is an extra hyperparameter all ES methods introduce. In contrast, stochastic forward mode method DODGE doesn't have such a hyperparameter and can instead always sample from the standard Gaussian distribution (i.e. $\sigma = 1$). Assuming the loss surface is locally quadratic, differentiable, and well-behaved, DODGE (with standard Gaussian distribution) would have similar variance properties as NRES and thus is a preferable choice than NRES among stochastic gradient estimation methods due to its lack of hyperparameters to tune.

Limitations of NRES as an Online method. Next we discuss two limitations of NRES as an *online* gradient estimation method for Unrolled Computation Graphs. The limitations are not specific to NRES but apply more broadly to classes of online methods.

- **[Hysteresis]** Any online gradient estimation methods (including TBPTT, DODGE, UORO, TES, PES, and NRES) would have bias due to hysteresis (see Section 2) because the parameter θ changes across adjacent partial online unrolls in the same UCG episode. Although we do not observe much impact of this bias in the applications considered in this paper, it is conceivable for some applications it could become an issue. In those cases, one should consider the tradeoffs of using NRES versus using Fulles – NRES allows more frequent gradient updates than Fulles while Fulles avoids the bias from hysteresis.
- **[T 's potential dependence on θ]** In this paper we assume the unrolled computation graph is of length T , where T doesn't depend on the value of the parameter θ . However, for some UCGs, an episode's length might be conditioned on what value of θ is used. For example, consider a robotic control problem where the robot could physically break when some action is taken. In this case, a prespecified episode length might not be reached. In Mujoco, these types of termination are called unhealthy conditions. This is potentially problematic for antithetic Online ES methods (including TES, PES, and NRES) when only one of the two antithetic (positive and negative) trajectories terminate early while not the other. In this case, if one directly resets both particles, one would ignore this useful information about the difference in antithetic directions. Besides, the early termination of some workers might also make all workers' truncation windows not uniformly distributed over the entire episode. How to gracefully handle these cases (through heuristics/principled approaches) would be an interesting question of future work to make online antithetic ES methods (especially NRES) more applicable for these problems.

Future Work. In future work, we are interested in exploring some natural open questions related to the above mentioned limitations: **1) choosing a sampling distribution for NRES.** Currently the isotropic variance σ^2 is tuned as a hyperparameter. Whether there are better ways to leverage the unrolled structure in the problem to further automate the selection of this distribution is an open question. **2) Incorporating hysteresis.** Our analysis assumes no hysteresis in the gradient estimates. However, understanding when and how to correct for hysteresis is an interesting direction. **3) Handling parameter-dependent episode length.** We hope to find a theoretically justified approach to handle the conditional episode length problem for NRES. This would allow principled application of NRES to on an even broader range of applications such as Reinforcement Learning tasks with early termination.

References

- Sepp Hochreiter and Jürgen Schmidhuber. Long short-term memory. *Neural Computation*, 9(8):1735–1780, 1997.
- Luke Metz, Niru Maheswaranathan, Jeremy Nixon, Daniel Freeman, and Jascha Sohl-Dickstein. Understanding and correcting pathologies in the training of learned optimizers. In *International Conference on Machine Learning*, 2019.
- Dougal Maclaurin, David Duvenaud, and Ryan Adams. Gradient-based hyperparameter optimization through reversible learning. In *International Conference on Machine Learning*, 2015.
- Tongzhou Wang, Jun-Yan Zhu, Antonio Torralba, and Alexei A Efros. Dataset distillation. *arXiv preprint arXiv:1811.10959*, 2018.
- Richard S Sutton, David McAllester, Satinder Singh, and Yishay Mansour. Policy gradient methods for reinforcement learning with function approximation. *Advances in Neural Information Processing Systems*, 1999.
- Atilim Gunes Baydin, Barak A Pearlmutter, Alexey Andreyevich Radul, and Jeffrey Mark Siskind. Automatic differentiation in machine learning: a survey. *Journal of Machine Learning Research*, 18:1–43, 2018.
- Tim Salimans, Jonathan Ho, Xi Chen, Szymon Sidor, and Ilya Sutskever. Evolution strategies as a scalable alternative to reinforcement learning. *arXiv preprint arXiv:1703.03864*, 2017.
- Paul Vicol, Luke Metz, and Jascha Sohl-Dickstein. Unbiased gradient estimation in unrolled computation graphs with persistent evolution strategies. In *International Conference on Machine Learning*, 2021.
- Paul Vicol, Zico Kolter, and Kevin Murphy. Low-variance gradient estimation in unrolled computation graphs with ES-Single. *arXiv preprint*, 2023.
- James Bradbury, Roy Frostig, Peter Hawkins, Matthew James Johnson, Chris Leary, Dougal Maclaurin, George Necula, Adam Paszke, Jake VanderPlas, Skye Wanderman-Milne, and Qiao Zhang. JAX: composable transformations of Python+NumPy programs, 2018. URL <http://github.com/google/jax>.
- Alex Beatson and Ryan P Adams. Efficient optimization of loops and limits with randomized telescoping sums. In *International Conference on Machine Learning*, 2019.
- Jeremy Cohen, Simran Kaur, Yuanzhi Li, J Zico Kolter, and Ameet Talwalkar. Gradient descent on neural networks typically occurs at the edge of stability. In *International Conference on Learning Representations*, 2021. URL <https://openreview.net/forum?id=jh-rTtvkGeM>.
- Peter W Glynn. Likelihood ratio gradient estimation for stochastic systems. *Communications of the ACM*, 33(10):75–84, 1990.
- Corentin Tallec and Yann Ollivier. Unbiased online recurrent optimization. *arXiv preprint arXiv:1702.05043*, 2017a.
- David Silver, Anirudh Goyal, Ivo Danihelka, Matteo Hessel, and Hado van Hasselt. Learning by directional gradient descent. In *International Conference on Learning Representations*, 2021.
- Pierre-Yves Massé and Yann Ollivier. Convergence of online adaptive and recurrent optimization algorithms. *arXiv preprint arXiv:2005.05645*, 2020.
- Chong Wang, Xi Chen, Alexander J Smola, and Eric P Xing. Variance reduction for stochastic gradient optimization. *Advances in neural information processing systems*, 26, 2013.

- Martín Abadi. Tensorflow: learning functions at scale. In *Proceedings of the 21st ACM SIGPLAN International Conference on Functional Programming*, pages 1–1, 2016.
- Adam Paszke, Sam Gross, Francisco Massa, Adam Lerer, James Bradbury, Gregory Chanan, Trevor Killeen, Zeming Lin, Natalia Gimelshein, Luca Antiga, et al. Pytorch: An imperative style, high-performance deep learning library. *Advances in Neural Information Processing Systems*, 2019.
- Tianqi Chen, Bing Xu, Chiyuan Zhang, and Carlos Guestrin. Training deep nets with sublinear memory cost. *arXiv preprint arXiv:1604.06174*, 2016.
- Corentin Tallec and Yann Ollivier. Unbiasing truncated backpropagation through time. *arXiv preprint arXiv:1705.08209*, 2017b.
- Aidan N Gomez, Mengye Ren, Raquel Urtasun, and Roger B Grosse. The reversible residual network: Backpropagation without storing activations. *Advances in Neural Information Processing Systems*, 2017.
- Yuhuai Wu, Mengye Ren, Renjie Liao, and Roger Grosse. Understanding short-horizon bias in stochastic meta-optimization. In *International Conference on Learning Representations*, 2018. URL <https://openreview.net/forum?id=H1MczcgR->.
- Ronald J Williams and David Zipser. A learning algorithm for continually running fully recurrent neural networks. *Neural Computation*, 1(2):270–280, 1989.
- Asier Mujika, Florian Meier, and Angelika Steger. Approximating real-time recurrent learning with random kronecker factors. *Advances in Neural Information Processing Systems*, 31, 2018.
- Frederik Benzing, Marcelo Matheus Gaury, Asier Mujika, Anders Martinsson, and Angelika Steger. Optimal kronecker-sum approximation of real time recurrent learning. In *International Conference on Machine Learning*, 2019.
- Peter I Frazier. A tutorial on bayesian optimization. *arXiv preprint arXiv:1807.02811*, 2018.
- James Bergstra and Yoshua Bengio. Random search for hyper-parameter optimization. *Journal of machine learning research*, 13(2), 2012.
- Alvaro Maggiar, Andreas Wachter, Irina S Dolinskaya, and Jeremy Staum. A derivative-free trust-region algorithm for the optimization of functions smoothed via gaussian convolution using adaptive multiple importance sampling. *SIAM Journal on Optimization*, 28(2):1478–1507, 2018.
- Guoqing Liu, Li Zhao, Feidiao Yang, Jiang Bian, Tao Qin, Nenghai Yu, and Tie-Yan Liu. Trust region evolution strategies. In *AAAI Conference on Artificial Intelligence*, 2019.
- Emanuel Todorov, Tom Erez, and Yuval Tassa. Mujoco: A physics engine for model-based control. In *International Conference on Intelligent Robots and Systems*, 2012.
- Krzysztof Choromanski, Mark Rowland, Vikas Sindhwani, Richard Turner, and Adrian Weller. Structured evolution with compact architectures for scalable policy optimization. In *International Conference on Machine Learning*, 2018.
- Niru Maheswaranathan, Luke Metz, George Tucker, Dami Choi, and Jascha Sohl-Dickstein. Guided evolutionary strategies: augmenting random search with surrogate gradients. In *International Conference on Machine Learning*, 2019.
- Alexandru Agapie. Spherical distributions used in evolutionary algorithms. *Mathematics*, 9(23), 2021. ISSN 2227-7390. doi: 10.3390/math9233098. URL <https://www.mdpi.com/2227-7390/9/23/3098>.
- Katelyn Gao and Ozan Sener. Generalizing Gaussian smoothing for random search. In *International Conference on Machine Learning*, 2022.

- Nikolaus Hansen. The cma evolution strategy: A tutorial. *arXiv preprint arXiv:1604.00772*, 2016.
- Yunhao Tang, Krzysztof Choromanski, and Alp Kucukelbir. Variance reduction for evolution strategies via structured control variates. In *International Conference on Artificial Intelligence and Statistics*, 2020.
- Luke Metz, James Harrison, C Daniel Freeman, Amil Merchant, Lucas Beyer, James Bradbury, Naman Agrawal, Ben Poole, Igor Mordatch, Adam Roberts, et al. Velo: Training versatile learned optimizers by scaling up. *arXiv preprint arXiv:2211.09760*, 2022a.
- Horia Mania, Aurelia Guy, and Benjamin Recht. Simple random search of static linear policies is competitive for reinforcement learning. In S. Bengio, H. Wallach, H. Larochelle, K. Grauman, N. Cesa-Bianchi, and R. Garnett, editors, *Advances in Neural Information Processing Systems*, volume 31. Curran Associates, Inc., 2018. URL https://proceedings.neurips.cc/paper_files/paper/2018/file/7634ea65a4e6d9041cfd3f7de18e334a-Paper.pdf.
- Dan Hendrycks and Kevin Gimpel. Gaussian error linear units (gelus). *arXiv preprint arXiv:1606.08415*, 2016.
- Han Xiao, Kashif Rasul, and Roland Vollgraf. Fashion-mnist: a novel image dataset for benchmarking machine learning algorithms. *arXiv preprint arXiv:1708.07747*, 2017.
- Greg Brockman, Vicki Cheung, Ludwig Pettersson, Jonas Schneider, John Schulman, Jie Tang, and Wojciech Zaremba. Openai gym. *arXiv preprint arXiv:1606.01540*, 2016.
- Luke Metz, C Daniel Freeman, James Harrison, Niru Maheswaranathan, and Jascha Sohl-Dickstein. Practical tradeoffs between memory, compute, and performance in learned optimizers. In *Conference on Lifelong Learning Agents (CoLLAs)*, 2022b. URL http://github.com/google/learned_optimization.

Appendix Outline

A. Notation

B. Algorithms

B.1 Online Evolution Strategies Pseudocode

B.2 Truncated Evolution Strategies Pseudocode

B.3 Noise-Reuse Evolution Strategies Pseudocode

C. Theory and Proofs

C.1 Proof of Lemma 1

C.2 Interpretation of Assumption 2

C.3 Proof of Lemma 4

C.4 Proof of Theorem 5

C.5 Proof of Corollary 6

C.6 Proof of Corollary 7

C.7 Proof of Theorem 8

D. Experiment Details

D.1 Hyperparameters

D.2 Additional Comparisons on the Learned Optimizers application

D.3 Computation resources needed

A Notation

In this section we provide two tables (Table 2 and 3) that summarize all the notations we use in the paper.

Table 2: Notations used in this paper (Part I)

T	the length of the unrolled computation graph
$[T]$	the set of integers $\{1, \dots, T\}$
$t \in \mathbb{Z} \cap [0, T]$	a time step of the dynamical system
$\theta \in \mathbb{R}^d$	the learnable parameter that unrolls the dynamical system at each time step
$\theta_i \in \mathbb{R}^d, i \in [T]$	the parameter that unrolls the dynamical system at the i -th time step
d	dimension of θ
$s \in \mathbb{R}^p$	the inner state of the dynamical system
$s_t \in \mathbb{R}^p$	the inner state of the dynamical system at time step t
p	the dimension of the inner state s in the dynamical system
$f_t : \mathbb{R}^p \times \mathbb{R}^d \rightarrow \mathbb{R}^d$	the transition dynamics from state at time step $t - 1$ to time step t . The state to be transitioned into at time step t is $f_t(s_{t-1}, \theta)$. f_t doesn't need to be the same for all $t \in [T]$. For example, different f_t could implicitly use different data as part of the computation.
$L_t^s : \mathbb{R}^p \rightarrow \mathbb{R}$	the loss function of the state s_t at time step $t \in [T]$, gives loss as $L_t^s(s_t)$.
$L_t : \mathbb{R}^{dt} \rightarrow \mathbb{R}$	the loss at time step $t \in [T]$ as a function of all the θ_i 's applied up to time step t , $L_t(\theta_1, \dots, \theta_t)$. Here θ_i doesn't need to be all the same.
$L : \mathbb{R}^{dT} \rightarrow \mathbb{R}$	the average loss over all T steps incurred by unrolling the system from s_0 to s_T using the sequence of $\{\theta_i\}_{i=1}^T$. $L(\theta_1, \dots, \theta_T) := \frac{1}{T} \sum_{t=1}^T L_t(\theta_1, \dots, \theta_t)$
$L_t([\theta]_{\times a}, [\theta']_{\times t-a})$	the loss incurred at time step t by first unrolling with θ for a steps, followed by unrolling with θ' for $t - a$ steps. $L_t([\theta]_{\times a}, [\theta']_{\times t-a}) := f(\underbrace{\theta, \dots, \theta}_a \text{ times}, \underbrace{\theta', \dots, \theta'}_{(t-a) \text{ times}})$
W	the length of an unroll truncation window (we always assume T is divisible by W for proof cleanness.)
$I_{d \times d}$	the d by d identity matrix
σ	a positive hyperparameter controlling the standard deviation in the isotropic Gaussian distribution $\mathcal{N}(\mathbf{0}, \sigma^2 I_{d \times d})$.
ϵ	a random perturbation vector in \mathbb{R}^d sampled from $\mathcal{N}(\mathbf{0}, \sigma^2 I_{d \times d})$
ϵ_i	the i -th Gaussian random vector sampled by an Online Evolution Strategies worker in a given episode. The total number of ϵ_i in an episode might be strictly smaller than the number of truncation windows (which is T/W) for GPES _{K} when $K > W$.
τ	a random variable sampled from the uniform distribution $\text{Unif}\{0, W, \dots, T - W\}$. τ denotes the starting time step of a truncation window by an Online Evolution Strategies worker.
K	the noise-sharing period for the algorithm GPES _{K} . K is always a multiple of W , i.e. $K = cW$ for some positive integer c .
c	the integer ratio K/W .

Table 3: Notations used in this paper (continued, Part II)

$\lceil x \rceil$	the ceiling of $x \in \mathbb{R}$, the smallest integer $y \in \mathbb{Z}$ such that $y \geq x$
$\lfloor x \rfloor$	the floor of $x \in \mathbb{R}$, the largest integer $y \in \mathbb{Z}$ such that $y \leq x$
$r : \mathbb{Z}^+ \times \mathbb{Z}^+ \rightarrow \mathbb{Z}^+$	the modified remainder function. $r(x, y)$ is the unique integer $n \in [1, y]$ where $x = qy + n$ for some integer q .
K -smoothed loss	the loss function: $\theta \mapsto \mathbb{E}_{\{\epsilon_i\}} L([\theta + \epsilon_1]_{\times K}, \dots, [\theta + \epsilon_{\lceil T/K \rceil}]_{\times r(T, K)})$.
$\{\{g_i^t \in \mathbb{R}^d\}_{i=1}^t\}_{t=1}^T$	the classes of sets of vectors associated with a given fixed θ defined in Assumption 2. For any given θ , there are T such sets of vectors, one for each time step $t \in \{1, \dots, T\}$. Roughly speaking, g_i^t is time step t 's smoothed loss's partial derivative with respect to the i -th application of θ
g^t	$g^t := \sum_{i=1}^t g_i^t$ for any time step t . Roughly speaking, g^t is time step t 's smoothed loss's total derivative with respect to the all the application of the same θ .
$g_{K,j}^t$	$g_{K,j}^t := \sum_{i=K \cdot (j-1)+1}^{\max\{t, K \cdot j\}} g_i^t$ for $j \in \{1, \dots, \lceil t/K \rceil\}$ and time step t . We can understand $g_{K,j}^t$ as the sum of partial derivatives of smoothed step- t loss with respect to all θ 's in the j -th noise-sharing window of size K . If K doesn't divide t , the last such window will be shorter than K .
$g_{c,j}^t$	$g_{K,j}^t$ when $K = c$ (used in the case of $W = 1$).
$\text{tr}(A)$	the trace (sum of diagonals) of a $d \times d$ matrix $A \in \mathbb{R}^{d \times d}$.
$\text{Cov}[\mathbf{X}]$	the $d \times d$ covariance matrix of random vector $\mathbf{X} \in \mathbb{R}^d$.
$\text{FullES}(\theta)$	a single FullES worker's gradient estimate given in Equation (3). To give a gradient estimate, the worker will run a total of $2T$ steps. The randomness comes from ϵ .
$\text{TES}(\theta)$	a single PES worker's gradient estimate given in Equation (4). This estimator keeps both a positive and negative inner state. To give a gradient estimate, the worker will run a total of $3W$ steps, one more W than PES because it needs to run unrolls also without perturbation. The randomness comes from $\{\epsilon_i\}_{i=1}^{T/W}$ and τ .
$\text{PES}(\theta)$	a single PES worker's gradient estimate given in Equation (6). This estimator keeps both a positive and negative inner state and samples a new noise perturbation at the beginning of every truncation window. A gradient estimate will run a total of $2W$ steps. The randomness comes from $\{\epsilon_i\}_{i=1}^{T/W}$ and τ .
$\text{GPES}_K(\theta)$	a single NRES worker's gradient estimate given in Lemma 1. This estimator keeps both a positive and negative inner state and samples a new noise perturbation every K steps in a given episode. To give a gradient estimate, the worker will run a total of $2W$ steps. The randomness comes from $\{\epsilon_i\}_{i=1}^{\lceil T/K \rceil}$ and τ .
$\text{NRES}(\theta)$	a single NRES worker's gradient estimate given. This is the same as $\text{GPES}_{K=T}(\theta)$. This estimator keeps both a positive and negative inner state, and it only samples a noise perturbation once at the beginning of an episode for each episode. To give a gradient estimate, the worker will run a total of $2W$ steps. The randomness comes from ϵ (single noise sampled at the beginning of an episode) and τ .

B Algorithms

In this section, we first provide Python-style pseudocode for the general Online Evolution Strategies training. We then provide the pseudocode for Truncated Evolution Strategies (TES) and Noise Reuse Evolution Strategies (NRES).

B.1 Online Evolution Strategies Pseudocode

OESWorker (Algorithm 3) is an abstract class (interface) that all the online ES methods will implement. The key functionality an OESWorker provides is its `worker.gradient_estimate(θ)` function that performs unrolls in a truncation window of size W and returns a gradient estimate based on the unroll. With this interface, we can train using online Evolution Strategies workers following Algorithm 4. The training takes two steps:

- Step 1. Constructing independent step-unlocked workers to form a worker pool. This requires sampling different truncation window starting point τ for different workers. During this stage, for simplicity and rigor, we only rely on the `.gradient_estimate` method call's side effect to alter the worker's saved states and discard the computed gradients. (We count these environment steps for the reinforcement learning experiment in Experiment 6.3.)
- Step 2. Training using the worker pool. At each outer iteration, we average all the worker's computed gradient estimates and pass that to any first order optimizer `OPT_UPDATE` (e.g. SGD or Adam) to update θ and repeat until convergence. Each worker's `gradient_estimate` method call can be parallelized.

Algorithm 3 Online Evolution Strategies (OES) (Abstract class)

```
import abc      # abstract base class
class OESWorker(abc.ABC):
    W: int      # the size of the truncation window
    @abc.abstractmethod
    def __init__(self, W):
        """
        set up the initial states with  $s_0$  and other bookkeeping variables
        """
        self.W = W
    @abc.abstractmethod
    def gradient_estimate(self,  $\theta$ ):
        """
        Given a  $\theta$ ,
        perform partial unroll in a truncation and return a gradient estimate for  $\theta$ 
        save the end inner state(s) and start off from the saved state(s)
        when .gradient_estimate is called again
        if reach the end, reset to initial states  $s_0$ 
        """
```

Algorithm 4 Training using Online Evolution Strategies

$\theta = \theta_{\text{init}}$ # start value of θ optimization.

Step 1: # Initialize OES workers

worker_list = []

for i **in** range(N): # N is the number of workers, can be parallelized

 new_worker = OESWorker(W) # replace with a real implementation of OESWorker

 # the steps below make sure the workers are step-unlocked

 # i.e. working independently at different truncation windows

$\tau \sim \text{Unif}\{0, W, \dots, T - W\}$

for t **in** range(τ/W):

$_ = \text{new_worker.gradient_estimate}(\theta)$

 worker_list.append(new_worker)

Step 2: # training

while not converged:

$g_{\text{sum}} = \mathbf{0}$ # g_{sum} is a vector in \mathbb{R}^d

for worker **in** worker_list: # can be parallelized

$g_{\text{sum}} += \text{worker.gradient_estimate}(\theta)$ # Add this worker's estimate

$g = g_{\text{sum}}/N$ # average all workers' gradient estimates

$\theta = \text{OPT_UPDATE}(\theta, g)$ # updating θ with any first order optimizers

return θ

B.2 Truncated Evolution Strategies Pseudocode

In Section 2, we have described the biased online Evolution Strategies method Truncated Evolution Strategies (TES). We have provided its analytical form:

$$\frac{1}{2\sigma^2 W} \sum_{i=1}^W [L_i([\theta]_{\times\tau}, [\theta + \epsilon]_{\times i}) - L_i([\theta]_{\times\tau}, [\theta - \epsilon]_{\times i})] \epsilon. \quad (13)$$

Here we provide the algorithm pseudocode for TES in Algorithm 5. It is important to note that after the antithetic unrolling using perturbed $\theta + \epsilon$ and $\theta - \epsilon$ for gradient estimates, another W steps of unrolling is done starting from the saved starting state using the unperturbed θ . The algorithm in this form is first introduced in [Vicol et al., 2021].

Algorithm 5 Truncated Evolution Strategies (TES)

class TESWorker(OESWorker):

def __init__(self, W):

 self. τ = 0; self. s = s_0 ; self. W = W

def gradient_estimate(self, θ):

$\epsilon \sim \mathcal{N}(\mathbf{0}, \sigma^2 I_{d \times d})$

$(s^+, s^-) = (\text{self}.s, \text{self}.s)$

$L_{\text{sum}}^+ = 0$; $L_{\text{sum}}^- = 0$

for i **in** range(1, self. W +1):

$s^+ = f_{\text{self}.\tau+i}(s^+, \theta + \epsilon)$; $s^- = f_{\text{self}.\tau+i}(s^-, \theta - \epsilon)$

$L_{\text{sum}}^+ += L_t^s(s^+)$; $L_{\text{sum}}^- += L_t^s(s^-)$

$g = (L_{\text{sum}}^+ - L_{\text{sum}}^-) / (2\sigma^2 \cdot \text{self}.W) \cdot \epsilon$

for i **in** range(1, self. W +1): # finally unroll using unperturbed θ

 self. $s = f_{\text{self}.\tau+i}(\text{self}.s, \theta)$;

 self. $\tau = \text{self}.\tau + W$

if self. $\tau \geq T$:

 # reset at the end of an episode

 self. $s = s_0$

 self. $\tau = 0$

return g

B.3 Noise-Reuse Evolution Strategies Pseudocode

Despite Noise Reuse Evolution Strategies being a special case of Generalized Persistent Evolution Strategies (GPES) whose algorithm is given in Algorithm 2, we provide NRES’s specific procedures in Algorithm 6. The simplifying change is that we only need to sample noise at the beginning of an episode (instead of every K steps) and we don’t need to keep track of the accumulated noise applied so far.

Algorithm 6 Noise-reuse Evolution Strategies (GPES)

class NRESWorker(OESWorker):

def __init__(self, W , K):

 self. τ = 0; self. s^+ = s_0 ; self. s^- = s_0
 self. W = W ; self. K = K

def gradient_estimate(self, θ):

 # only sample a new ϵ at the beginning of an episode

if self. τ == 0:

$\epsilon \sim \mathcal{N}(\mathbf{0}, \sigma^2 I_{d \times d})$

 # keep track of ϵ to use for this entire episode

 self. ϵ = ϵ

 (s^+ , s^-) = (self. s^+ , self. s^-)

$L_{\text{sum}}^+ = 0$; $L_{\text{sum}}^- = 0$

for i **in** range(1, self. W +1):

$s^+ = f_{\text{self.}\tau+i}(s^+, \theta + \text{self.}\epsilon)$

$s^- = f_{\text{self.}\tau+i}(s^-, \theta - \text{self.}\epsilon)$

$L_{\text{sum}}^+ += L_{\text{self.}\tau+i}^s(s^+)$; $L_{\text{sum}}^- += L_{\text{self.}\tau+i}^s(s^-)$

$g = (L_{\text{sum}}^+ - L_{\text{sum}}^-) / (2\sigma^2 \cdot \text{self.}W) \cdot \text{self.}\epsilon$ # not self. ξ

 self. $s^+ = s^+$; self. $s^- = s^-$

 self. τ = self. τ + W

if self. τ $\geq T$:

 # reset at the end of an episode

 self. τ = 0; self. $s^+ = s_0$; self. $s^- = s_0$

return g

C Theory and Proofs

In this section, we provide the proofs and interpretations of the lemmas, assumptions, and theorems presented in the main paper and restate these results for completeness. Before we begin, we define some background and notation:

- We treat all real-valued function's gradient as column vectors.
- We use $[\theta]_{\times t}$ to denote t copies to θ stacked together to form a td -dimensional column vector.
- For $\{v_i \in \mathbb{R}^d\}_{i=1}^m$, we use $\begin{bmatrix} v_1 \\ \vdots \\ v_m \end{bmatrix}$ to denote the column vector whose first d -dimensions is v_1 and so on and so forth. Similar we use $[v_1 \ \dots \ v_m]$ to denote the transpose of the previous vector (thus a row vector).
- **Gradient notation** For any real-valued function whose input is more than one single θ (for example L_t takes in t number of θ 's), we will use ∇_{Θ} to describe the gradient with respect to the function's entire input dimension and similarly ∇_{Θ}^2 for Hessian. For such functions, we will use $\frac{\partial}{\partial \theta_i}$ to denote the partial derivative of the function with respect to the i -th θ . We will use $\frac{d}{d\theta}$ to define the total derivative of some variable with respect to θ (e.g. when talking about $\frac{dL_{\text{avg}}}{d\theta}$ with $L_{\text{avg}}(\theta) := L([\theta]_{\times t})$ if L is differentiable). This notation will also describe the Jacobian matrix when the output function is vector-valued.

C.1 Proof of Lemma 1

Define the K -smoothed loss objective as the function:

$$\theta \mapsto \mathbb{E}_{\{\epsilon_i\}} L([\theta + \epsilon_1]_{\times K}, \dots, [\theta + \epsilon_{\lceil T/K \rceil}]_{\times r(T, K)}). \quad (14)$$

Lemma 1. *An unbiased gradient estimator for the K -smoothed loss is given by*

$$\text{GPES}_{K=cW}(\theta) \quad (15)$$

$$\begin{aligned} &:= \frac{1}{2\sigma^2 W} \sum_{j=1}^W \left[L_{\tau+j}([\theta + \epsilon_1]_{\times K}, [\theta + \epsilon_2]_{\times K}, \dots, [\theta + \epsilon_{\lceil \tau/K \rceil + 1}]_{\times r(\tau+j, K)}) \right. \\ &\quad \left. - L_{\tau+j}([\theta - \epsilon_1]_{\times K}, [\theta - \epsilon_2]_{\times K}, \dots, [\theta - \epsilon_{\lceil \tau/K \rceil + 1}]_{\times r(\tau+j, K)}) \right] \cdot \left(\sum_{i=1}^{\lceil \tau/K \rceil + 1} \epsilon_i \right), \quad (16) \end{aligned}$$

with randomness in $\tau \sim \text{Unif}\{0, W, \dots, T - W\}$ and $\{\epsilon_i\}_{i=1}^{\lceil T/K \rceil} \stackrel{\text{iid}}{\sim} \mathcal{N}(\mathbf{0}, \sigma^2 I_{d \times d})$.

Proof.

For simplicity, we will denote $q = \lceil T/K \rceil$ and $r = r(T, K)$.

First let's define a function $L^K : \mathbb{R}^{d \cdot q} \rightarrow \mathbb{R}$

$$L^K(\theta_1, \dots, \theta_q) := L([\theta_1]_{\times K}, \dots, [\theta_{q-1}]_{\times K}, [\theta_q]_{\times r}), \quad (17)$$

and a smoothed version of L^K by $\widehat{L}^K : \mathbb{R}^{d \cdot q} \rightarrow \mathbb{R}$ with

$$\widehat{L}^K(\theta_1, \dots, \theta_q) := \mathbb{E}_{\{\epsilon_i\}_{i=1}^q} L^K(\theta_1 + \epsilon_1, \dots, \theta_q + \epsilon_q). \quad (18)$$

We notice that by definition, the K -smoothed loss function can be expressed as

$$\theta \mapsto \widehat{L}^K([\theta]_{\times q}). \quad (19)$$

In this form, the K -smoothed loss function is a simple composition of two functions: the first function maps θ to q -times repetition of $[\theta]_{\times q}$, while the second function is exactly \widehat{L}^K . For the first vector-valued function, we see that its Jacobian is given by:

$$\frac{d}{d\theta}(\theta \mapsto [\theta]_{\times q}) = \mathbf{1}_q \otimes I_{d \times d} \in \mathbb{R}^{q \times d}, \quad (20)$$

where $\mathbf{1}_q \in \mathbb{R}^q$ is a vector of 1's and $\otimes(\cdot, \cdot)$ is the Kronecker product operator. For the second function, we see that by the score function gradient estimator trick [Glynn, 1990],

$$\nabla_{\Theta} \widehat{L}^K(\theta_1, \dots, \theta_q) = \frac{1}{\sigma^2} \mathbb{E}_{\{\epsilon_i\}_{i=1}^q} L^K(\theta_1 + \epsilon_1, \dots, \theta_q + \epsilon_q) \begin{bmatrix} \epsilon_1 \\ \vdots \\ \epsilon_q \end{bmatrix}. \quad (21)$$

Now we are ready to compute the gradient of the K -smoothed loss using chain rule (recall that we assume the gradients are column vectors):

$$\nabla_{\theta} \left(\theta \mapsto \widehat{L}^K([\theta]_{\times q}) \right) \quad (22)$$

$$= \left[\frac{d}{d\theta}(\theta \mapsto [\theta]_{\times q}) \right]^{\top} \nabla_{\Theta} \widehat{L}^K \Big|_{\Theta=[\theta]_{\times q}} \quad (23)$$

$$= (\mathbf{1}_q \otimes I_{d \times d})^{\top} \mathbb{E}_{\{\epsilon_i\}_{i=1}^q} \frac{1}{\sigma^2} L^K(\theta + \epsilon_1, \dots, \theta + \epsilon_q) \begin{bmatrix} \epsilon_1 \\ \vdots \\ \epsilon_q \end{bmatrix} \quad (24)$$

$$= \frac{1}{\sigma^2} \mathbb{E}_{\{\epsilon_i\}_{i=1}^q} L^K(\theta + \epsilon_1, \dots, \theta + \epsilon_q) \left((\mathbf{1}_q \otimes I_{d \times d})^{\top} \begin{bmatrix} \epsilon_1 \\ \vdots \\ \epsilon_q \end{bmatrix} \right) \quad (25)$$

$$= \frac{1}{\sigma^2} \mathbb{E}_{\{\epsilon_i\}_{i=1}^q} L^K(\theta + \epsilon_1, \dots, \theta + \epsilon_q) \left(\sum_{i=1}^q \epsilon_i \right). \quad (26)$$

Here the last step is by the algebra of Kronecker product. With this, we now consider the structure of L^K as an average of losses over all time steps by converting this average into an expectation over truncation windows starting at τ :

$$\nabla_{\theta} \left(\theta \mapsto \widehat{L}^K([\theta]_{\times q}) \right) \quad (27)$$

$$= \frac{1}{\sigma^2} \mathbb{E}_{\{\epsilon_i\}_{i=1}^q} L^K(\theta + \epsilon_1, \dots, \theta + \epsilon_q) \left(\sum_{i=1}^q \epsilon_i \right) \quad (28)$$

$$= \frac{1}{\sigma^2} \mathbb{E}_{\{\epsilon_i\}_{i=1}^q} \frac{1}{T} \sum_{t=1}^T L_t([\theta + \epsilon_1]_{\times K}, [\theta + \epsilon_2]_{\times K} \dots, [\theta + \epsilon_{\lceil t/K \rceil}]_{\times r(t,K)}) \left(\sum_{i=1}^q \epsilon_i \right) \quad (29)$$

$$= \frac{1}{\sigma^2} \mathbb{E}_{\{\epsilon_i\}_{i=1}^q} \frac{1}{T/W} \sum_{b=0}^{T/W-1} \frac{1}{W} \sum_{j=1}^W L_{Wb+j}([\theta + \epsilon_1]_{\times K}, [\theta + \epsilon_2]_{\times K} \dots, [\theta + \epsilon_{\lceil (Wb+j)/K \rceil}]_{\times r(Wb+j,K)}) \left(\sum_{i=1}^q \epsilon_i \right) \quad (30)$$

$$= \frac{1}{\sigma^2} \mathbb{E}_{\{\epsilon_i\}_{i=1}^q} \frac{1}{T/W} \sum_{b=0}^{T/W-1} \frac{1}{W} \sum_{j=1}^W L_{Wb+j}([\theta + \epsilon_1]_{\times K}, [\theta + \epsilon_2]_{\times K} \dots, [\theta + \epsilon_{\lfloor Wb/K \rfloor + 1}]_{\times r(Wb+j,K)}) \left(\sum_{i=1}^q \epsilon_i \right) \quad (31)$$

Here the last step we observe that $\lceil (Wb+j)/K \rceil = \lfloor Wb/K \rfloor + 1$ for any $1 \leq j \leq W \leq K$.

Here we notice that for Equation 31, when $\lfloor Wb/K \rfloor + 1 < i$, there is independence between the random vector ϵ_i and the term $L_{Wb+j}([\theta + \epsilon_1]_{\times K}, [\theta + \epsilon_2]_{\times K} \dots, [\theta + \epsilon_{\lfloor Wb/K \rfloor + 1}]_{\times r(Wb+j,K)})$. The expectation of the product between these independent terms is then $\mathbf{0}$ because $\mathbb{E}[\epsilon_i] = \mathbf{0}$. As a result, we have the further simplification:

$$\nabla_{\theta} \left(\theta \mapsto \widehat{L}^K([\theta]_{\times q}) \right) \quad (32)$$

$$= \frac{1}{\sigma^2} \mathbb{E}_{\{\epsilon_i\}_{i=1}^q} \left[\frac{1}{T/W} \sum_{b=0}^{T/W-1} \frac{1}{W} \sum_{j=1}^W L_{Wb+j}([\theta + \epsilon_1]_{\times K}, [\theta + \epsilon_2]_{\times K} \dots, [\theta + \epsilon_{\lfloor Wb/K \rfloor + 1}]_{\times r(Wb+j,K)}) \left(\sum_{i=1}^{\lfloor Wb/K \rfloor + 1} \epsilon_i \right) \right] \quad (33)$$

$$= \frac{1}{\sigma^2} \mathbb{E}_{\{\epsilon_i\}_{i=1}^q} \mathbb{E}_{\tau} \frac{1}{W} \sum_{j=1}^W L_{\tau+j}([\theta + \epsilon_1]_{\times K}, [\theta + \epsilon_2]_{\times K} \dots, [\theta + \epsilon_{\lfloor \tau/K \rfloor + 1}]_{\times r(\tau+j,K)}) \left(\sum_{i=1}^{\lfloor \tau/K \rfloor + 1} \epsilon_i \right). \quad (34)$$

Here the last step converts the average in Equation 33 into an expectation in Equation 34 by treating Wb as the random variable τ . By additionally averaging over the antithetic samples of the random variable in Equation 34, we arrive the unbiased estimator in the Lemma thus completing the proof. \square

C.2 Interpretation of Assumption 2

Assumption 2. For a given fixed $\theta \in \mathbb{R}^d$, for any $t \in [T]$, there exists a set of vectors $\{g_i^t \in \mathbb{R}^d\}_{i=1}^t$, such that for any $\{v_i \in \mathbb{R}^d\}_{i=1}^t$, the following equality holds:

$$L_t(\theta + v_1, \theta + v_2, \dots, \theta + v_t) - L_t(\theta - v_1, \theta - v_2, \dots, \theta - v_t) = 2 \sum_{i=1}^t (v_i)^\top (g_i^t) \quad (35)$$

Here we show that when $L_t : \mathbb{R}^{dt} \rightarrow \mathbb{R}$ is a quadratic function, this assumption would hold with $g_i^t = \frac{\partial L_t}{\partial \theta_i}$.

If L_t is a quadratic (assumption made in [Vicol et al., 2021]), it can be expressed exactly as its second-order Taylor expansion. Then we have

$$L_t(\theta + v_1, \theta + v_2, \dots, \theta + v_t) = L_t([\theta]_{\times t}) + \left(\nabla_{\Theta} L_t \Big|_{\Theta=[\theta]_{\times t}} \right)^{\top} \begin{bmatrix} v_1 \\ \vdots \\ v_t \end{bmatrix} + \frac{1}{2} [v_1 \quad \dots \quad v_t] \nabla_{\Theta}^2 L_t \begin{bmatrix} v_1 \\ \vdots \\ v_t \end{bmatrix} \quad (36)$$

$$L_t(\theta - v_1, \theta - v_2, \dots, \theta - v_t) = L_t([\theta]_{\times t}) - \left(\nabla_{\Theta} L_t \Big|_{\Theta=[\theta]_{\times t}} \right)^{\top} \begin{bmatrix} v_1 \\ \vdots \\ v_t \end{bmatrix} + \frac{1}{2} [v_1 \quad \dots \quad v_t] \nabla_{\Theta}^2 L_t \begin{bmatrix} v_1 \\ \vdots \\ v_t \end{bmatrix} \quad (37)$$

Taking the difference of the above two equations, we have that

$$L_t(\theta + v_1, \theta + v_2, \dots, \theta + v_t) - L_t(\theta - v_1, \theta - v_2, \dots, \theta - v_t) = 2 \left(\nabla_{\Theta} L_t \Big|_{\Theta=[\theta]_{\times t}} \right)^{\top} \begin{bmatrix} v_1 \\ \vdots \\ v_t \end{bmatrix}. \quad (38)$$

We note that

$$\nabla_{\Theta} L_t \Big|_{\Theta=[\theta]_{\times t}} = \begin{bmatrix} \frac{\partial L_t}{\partial \theta_1} \\ \vdots \\ \frac{\partial L_t}{\partial \theta_t} \end{bmatrix}. \quad (39)$$

Plugging it into Equation (37), we have

$$L_t(\theta + v_1, \theta + v_2, \dots, \theta + v_t) - L_t(\theta - v_1, \theta - v_2, \dots, \theta - v_t) = 2 \sum_{i=1}^t v_i^{\top} \frac{\partial L_t}{\partial \theta_i}. \quad (40)$$

Thus we see in the case of quadratic L_t , g_i^t is just the partial derivative of L_t with respect to θ_i (i.e., $\frac{\partial L_t}{\partial \theta_i}$). Hence we see that our assumptions generalize those made in [Vicol et al., 2021].

C.3 Proof of Lemma 4

Lemma 4. Under Assumption 2, when $W = 1$, $\text{GPES}_{K=c}(\theta) = \frac{1}{\sigma^2} \sum_{j=1}^{\lfloor \tau/c \rfloor + 1} \left(\sum_{i=1}^{\lfloor \tau/c \rfloor + 1} \epsilon_i \right) \epsilon_j^\top g_{c,j}^\tau$, where the randomness lies in $\tau \sim \text{Unif}\{0, 1, \dots, T-1\}$ and $\{\epsilon_i\} \stackrel{\text{iid}}{\sim} \mathcal{N}(\mathbf{0}, \sigma^2 I_{d \times d})$.

Proof. We see that when $W = 1$,

$$\text{GPES}_{K=c}(\theta) \tag{41}$$

$$= \frac{1}{2\sigma^2 W} \sum_{j=1}^{W=1} \left[L_{\tau+j}([\theta + \epsilon_1]_{\times K}, [\theta + \epsilon_2]_{\times K}, \dots, [\theta + \epsilon_{\lfloor \tau/K \rfloor + 1}]_{\times r(\tau+j, K)}) \right. \\ \left. - L_{\tau+j}([\theta - \epsilon_1]_{\times K}, [\theta - \epsilon_2]_{\times K}, \dots, [\theta - \epsilon_{\lfloor \tau/K \rfloor + 1}]_{\times r(\tau+j, K)}) \right] \cdot \left(\sum_{i=1}^{\lfloor \tau/K \rfloor + 1} \epsilon_i \right) \tag{42}$$

$$= \frac{1}{2\sigma^2} \left[L_{\tau+1}([\theta + \epsilon_1]_{\times c}, [\theta + \epsilon_2]_{\times c}, \dots, [\theta + \epsilon_{\lfloor \tau/c \rfloor + 1}]_{\times r(\tau+1, c)}) \right. \\ \left. - L_{\tau+1}([\theta - \epsilon_1]_{\times c}, [\theta - \epsilon_2]_{\times c}, \dots, [\theta - \epsilon_{\lfloor \tau/c \rfloor + 1}]_{\times r(\tau+1, c)}) \right] \cdot \left(\sum_{i=1}^{\lfloor \tau/c \rfloor + 1} \epsilon_i \right) \tag{43}$$

Applying Assumption 2 to the difference in the last equation, we have

$$L_{\tau+1}([\theta + \epsilon_1]_{\times c}, [\theta + \epsilon_2]_{\times c}, \dots, [\theta + \epsilon_{\lfloor \tau/c \rfloor + 1}]_{\times r(\tau+1, c)}) \\ - L_{\tau+1}([\theta - \epsilon_1]_{\times c}, [\theta - \epsilon_2]_{\times c}, \dots, [\theta - \epsilon_{\lfloor \tau/c \rfloor + 1}]_{\times r(\tau+1, c)}) \tag{44}$$

$$= 2 \sum_{j=1}^{\lfloor \tau/c \rfloor + 1} \left[\epsilon_j^\top \left(\sum_{i=c \cdot (j-1) + 1}^{\min\{\tau+1, c \cdot j\}} g_i^{\tau+1} \right) \right] \tag{45}$$

$$= 2 \sum_{j=1}^{\lfloor \tau/c \rfloor + 1} \epsilon_j^\top g_{c,j}^{\tau+1} \tag{46}$$

Plugging this equality in to Equation 43, we get

$$\text{GPES}_{K=c}(\theta) = \frac{1}{\sigma^2} \sum_{j=1}^{\lfloor \tau/c \rfloor + 1} \left(\sum_{i=1}^{\lfloor \tau/c \rfloor + 1} \epsilon_i \right) \epsilon_j^\top g_{c,j}^{\tau+1}$$

□

C.4 Proof of Theorem 5

Theorem 5. When $W = 1$ and under Assumption 2, the total variance of $\text{GPES}_{K=c}(\theta)$ has the following form for any integer $c \in [1, T]$,

$$\text{tr}(\text{Cov}[\text{GPES}_{K=c}(\theta)]) = \frac{(d+2)}{T} \sum_{t=1}^T (\|g^t\|_2^2) - \left\| \frac{1}{T} \sum_{t=1}^T g^t \right\|_2^2 + \frac{1}{T} \sum_{t=1}^T \left(\frac{d}{2} \sum_{j=1, j' \neq 1}^{\lceil t/c \rceil} \|g_{c,j}^t - g_{c,j'}^t\|_2^2 \right). \quad (47)$$

Proof. First we break down the total variance:

$$\text{tr}(\text{Cov}[\text{GPES}_{K=c}(\theta)]) \quad (48)$$

$$= \text{tr}(\mathbb{E} \left[(\text{GPES}_{K=c}(\theta) - \mathbb{E}[\text{GPES}_{K=c}(\theta)]) (\text{GPES}_{K=c}(\theta) - \mathbb{E}[\text{GPES}_{K=c}(\theta)])^\top \right]) \quad (49)$$

$$= \text{tr}(\mathbb{E} \text{GPES}_{K=c}(\theta) \text{GPES}_{K=c}(\theta)^\top) - \text{tr}(\mathbb{E} \text{GPES}_{K=c}(\theta) [\mathbb{E} \text{GPES}_{K=c}(\theta)]^\top) \quad (50)$$

$$= (\mathbb{E} \text{tr}[\text{GPES}_{K=c}(\theta) \text{GPES}_{K=c}(\theta)^\top]) - [\mathbb{E} \text{GPES}_{K=c}(\theta)]^\top [\mathbb{E} \text{GPES}_{K=c}(\theta)] \quad (51)$$

$$= \mathbb{E} \|\text{GPES}_{K=c}(\theta)\|_2^2 - \|\mathbb{E} \text{GPES}_{K=c}(\theta)\|_2^2 \quad (52)$$

$$= \mathbb{E}_{\boldsymbol{\tau}} \mathbb{E}_{\{\epsilon_i\} | \boldsymbol{\tau} = t-1} \|\text{GPES}_{K=c}(\theta)\|_2^2 - \|\mathbb{E} \text{GPES}_{K=c}(\theta)\|_2^2 \quad (53)$$

$$= \frac{1}{T} \sum_{t=1}^T \underbrace{\mathbb{E}_{\{\epsilon_i\} | \boldsymbol{\tau} = t-1} \|\text{GPES}_{K=c}(\theta)\|_2^2}_{\textcircled{1}} - \underbrace{\|\mathbb{E} \text{GPES}_{K=c}(\theta)\|_2^2}_{\textcircled{2}} \quad (54)$$

Thus to analytically express the trace of covariance, we need to separately derive $\textcircled{1}$ for any $t \in \{1, \dots, T\}$ and $\textcircled{2}$.

$\textcircled{1}$ Expressing $\mathbb{E}_{\{\epsilon_i\} | \boldsymbol{\tau} = t-1} \|\text{GPES}_{K=c}(\theta)\|_2^2$.

Here we see that for a given $t \in [T]$, conditioning on $\boldsymbol{\tau} = t-1$, we have

$$\frac{1}{\sigma^2} \sum_{j=1}^{\lfloor \boldsymbol{\tau}/c \rfloor + 1} \left(\sum_{i=1}^{\lfloor \boldsymbol{\tau}/c \rfloor + 1} \epsilon_i \right) \epsilon_j^\top g_{c,j}^{\boldsymbol{\tau}+1} \quad (55)$$

$$= \frac{1}{\sigma^2} \sum_{j=1}^{\lfloor (t-1)/c \rfloor + 1} \left(\sum_{i=1}^{\lfloor (t-1)/c \rfloor + 1} \epsilon_i \right) \epsilon_j^\top g_{c,j}^t \quad (56)$$

$$= \frac{1}{\sigma^2} \sum_{j=1}^{\lceil t/c \rceil} \left(\sum_{i=1}^{\lceil t/c \rceil} \epsilon_i \right) \epsilon_j^\top g_{c,j}^t, \quad (57)$$

where in the last step we use the fact that for integer t , $\lfloor (t-1)/c \rfloor + 1 = \lceil t/c \rceil$. Because we are deriving expression $\textcircled{1}$ for every value of t separately, to simplify the notation, we define $n := \lceil t/c \rceil$ and $a_j := g_{c,j}^t$ for a given fixed t .

Then the expression in Equation (57) can be simplified as $\frac{1}{\sigma^2} \sum_{j=1}^n (\sum_{i=1}^n \epsilon_i) \epsilon_j^\top a_j$.

As a result, term ① can be expressed as

$$\mathbb{E}_{\{\epsilon\}|\tau=t-1} \|\text{GPES}_{K=c}(\theta)\|_2^2 \quad (58)$$

$$= \mathbb{E}_{\epsilon} \left\| \frac{1}{\sigma^2} \sum_{j=1}^n \left(\sum_{i=1}^n \epsilon_i \right) \epsilon_j^\top a_j \right\|_2^2 \quad (59)$$

$$= \frac{1}{\sigma^4} \mathbb{E}_{\epsilon} \left[\sum_{i=1}^n \left(\sum_{k=1}^n \epsilon_k \right) \epsilon_i^\top a_i \right]^\top \left[\sum_{j=1}^n \left(\sum_{l=1}^n \epsilon_l \right) \epsilon_j^\top a_j \right] \quad (60)$$

$$= \frac{1}{\sigma^4} \sum_{i=1}^n \sum_{j=1}^n a_i^\top \mathbb{E}_{\epsilon} \left[\epsilon_i \left(\sum_{k=1}^n \epsilon_k \right)^\top \left(\sum_{l=1}^n \epsilon_l \right) \epsilon_j^\top \right] a_j \quad (61)$$

$$= \frac{1}{\sigma^4} \sum_{i=1}^n \sum_{j=1}^n \left(\left[\sum_{k=1}^n \sum_{l=1}^n \mathbb{E}_{\epsilon} \epsilon_i \epsilon_k^\top \epsilon_l \epsilon_j^\top \right] \right) a_i^\top a_j \quad (62)$$

From Equation (62), we see that term ① is a quadratic in $\{a_i\}_{i=1}^n$ with each pairwise inner product's coefficient determined by an expectation. Thus we break into different cases to evaluate the expectation $[\sum_{k=1}^n \sum_{l=1}^n \mathbb{E}_{\epsilon} \epsilon_i \epsilon_k^\top \epsilon_l \epsilon_j^\top]$ for different values of i, j, k, l .

Begin of Cases

Case (I) $i = j$.

(I.1) If $k \neq i, l \neq i$,

$$\begin{aligned} & \mathbb{E}_{\epsilon} \epsilon_i \epsilon_k^\top \epsilon_l \epsilon_j^\top \\ &= \mathbb{E}_{\epsilon_i, \epsilon_k, \epsilon_l} \epsilon_i \epsilon_k^\top \epsilon_l \epsilon_i^\top \\ &= \mathbb{E}_{\epsilon_i} \mathbb{E}_{\epsilon_k, \epsilon_l} \epsilon_i \epsilon_k^\top \epsilon_l \epsilon_i^\top \\ &= \mathbb{E}_{\epsilon_i} \epsilon_i [\mathbb{E}_{\epsilon_k, \epsilon_l} \epsilon_k^\top \epsilon_l] \epsilon_i^\top \end{aligned}$$

(I.1.a) If $k \neq i, l \neq i$, and $k \neq l$, then $\mathbb{E}_{\epsilon_k, \epsilon_l} \epsilon_k^\top \epsilon_l = 0$ and $E_{\epsilon} \epsilon_i \epsilon_k^\top \epsilon_l \epsilon_j^\top = \mathbf{0}$.

(I.1.b) If $k \neq i, l \neq i$, and $k = l$.

$$\begin{aligned} & \mathbb{E}_{\epsilon_i} \epsilon_i [\mathbb{E}_{\epsilon_k, \epsilon_l} \epsilon_k^\top \epsilon_l] \epsilon_i^\top \\ &= \mathbb{E}_{\epsilon_i} \epsilon_i [\mathbb{E}_{\epsilon_k} \epsilon_k^\top \epsilon_k] \epsilon_i^\top \\ &= (d\sigma^2) \sigma^2 I_d \\ &= d\sigma^4 I_d \end{aligned}$$

(I.2) If $k = i, l \neq i$,

$$\begin{aligned} & \mathbb{E}_{\epsilon} \epsilon_i \epsilon_k^\top \epsilon_l \epsilon_j^\top \\ &= \mathbb{E}_{\epsilon} \epsilon_i \epsilon_i^\top \epsilon_l \epsilon_i^\top \\ &= \mathbb{E}_{\epsilon_i} \epsilon_i \epsilon_i^\top \mathbb{E}_{\epsilon_l} [\epsilon_l] \epsilon_i^\top \\ &= \mathbf{0} \end{aligned}$$

(I.3) If $k \neq i, l = i$, similarly as **(I.2)**,

$$\begin{aligned}
& \mathbb{E}_{\boldsymbol{\epsilon}} \boldsymbol{\epsilon}_i \boldsymbol{\epsilon}_k^\top \boldsymbol{\epsilon}_l \boldsymbol{\epsilon}_j^\top \\
&= \mathbb{E}_{\boldsymbol{\epsilon}} \boldsymbol{\epsilon}_i \boldsymbol{\epsilon}_k^\top \boldsymbol{\epsilon}_i \boldsymbol{\epsilon}_i^\top \\
&= \mathbb{E}_{\boldsymbol{\epsilon}_i} \boldsymbol{\epsilon}_i \mathbb{E}_{\boldsymbol{\epsilon}_k} [\boldsymbol{\epsilon}_k^\top] \boldsymbol{\epsilon}_i \boldsymbol{\epsilon}_i^\top \\
&= \mathbf{0}
\end{aligned}$$

(I.4) If $k = i, l = i$, by Isserlis' theorem (derivation see [Maheswaranathan et al., 2019] Supplementary material A.2),

$$\begin{aligned}
& \mathbb{E}_{\boldsymbol{\epsilon}} \boldsymbol{\epsilon}_i \boldsymbol{\epsilon}_k^\top \boldsymbol{\epsilon}_l \boldsymbol{\epsilon}_j^\top \\
&= \mathbb{E}_{\boldsymbol{\epsilon}_i} \boldsymbol{\epsilon}_i \boldsymbol{\epsilon}_i^\top \boldsymbol{\epsilon}_i \boldsymbol{\epsilon}_i^\top \\
&= (d+2) \sigma^4 I_d
\end{aligned}$$

Combining **(I.1)** to **(I.4)**, we see that for the case of $i = j$,

$$\sum_{k=1}^n \sum_{l=1}^n \mathbb{E}_{\boldsymbol{\epsilon}} \boldsymbol{\epsilon}_i \boldsymbol{\epsilon}_k^\top \boldsymbol{\epsilon}_l \boldsymbol{\epsilon}_j^\top = \left[\sum_{k \neq i} d \sigma^4 I_d \right] + (d+2) \sigma^4 I_d = (td+2) \sigma^4 I_d \quad (63)$$

Case (II) $i \neq j$.

(II.1) $k \neq i, k \neq j$.

(II.1.a) If $k \neq i, k \neq j$, and additionally $k \neq l$,

$$\begin{aligned}
& \mathbb{E}_{\boldsymbol{\epsilon}} \boldsymbol{\epsilon}_i \boldsymbol{\epsilon}_k^\top \boldsymbol{\epsilon}_l \boldsymbol{\epsilon}_j^\top \\
&= \mathbb{E}_{\boldsymbol{\epsilon}_i, \boldsymbol{\epsilon}_j, \boldsymbol{\epsilon}_l} \boldsymbol{\epsilon}_i (\mathbb{E}_{\boldsymbol{\epsilon}_k} [\boldsymbol{\epsilon}_k])^\top \boldsymbol{\epsilon}_l \boldsymbol{\epsilon}_j^\top \\
&= \mathbf{0}
\end{aligned}$$

(II.1.b) If $k \neq i, k \neq j$, and $k = l$,

After pulling out $\mathbb{E}_{\boldsymbol{\epsilon}_k} [\boldsymbol{\epsilon}_k^\top \boldsymbol{\epsilon}_k]$, because $i \neq j$, we still have the expectation = 0.

$$\begin{aligned}
& \mathbb{E}_{\boldsymbol{\epsilon}} \boldsymbol{\epsilon}_i \boldsymbol{\epsilon}_k^\top \boldsymbol{\epsilon}_l \boldsymbol{\epsilon}_j^\top \\
&= \mathbb{E}_{\boldsymbol{\epsilon}} \boldsymbol{\epsilon}_i \mathbb{E} [\boldsymbol{\epsilon}_k^\top \boldsymbol{\epsilon}_k] \boldsymbol{\epsilon}_j^\top \\
&= [\mathbb{E}_{\boldsymbol{\epsilon}_i, \boldsymbol{\epsilon}_j} \boldsymbol{\epsilon}_i \boldsymbol{\epsilon}_j^\top] \cdot \mathbb{E} [\boldsymbol{\epsilon}_k^\top \boldsymbol{\epsilon}_k] \\
&= \mathbf{0} \cdot \mathbb{E} [\boldsymbol{\epsilon}_k^\top \boldsymbol{\epsilon}_k] \\
&= \mathbf{0}
\end{aligned}$$

(II.2) $k = i$,

(II.2.a) if $l \neq i, l \neq j$. This is similar to **(II.1)** as we can swap the position of k and j in the expression:

$$\boldsymbol{\epsilon}_i \boldsymbol{\epsilon}_k^\top \boldsymbol{\epsilon}_l \boldsymbol{\epsilon}_j^\top = \boldsymbol{\epsilon}_i \boldsymbol{\epsilon}_l^\top \boldsymbol{\epsilon}_k \boldsymbol{\epsilon}_j^\top.$$

Thus we have $\mathbb{E}_{\epsilon} \epsilon_i \epsilon_k^\top \epsilon_l \epsilon_j^\top = \mathbf{0}$.

(II.2.b) if $l = i$,

$$\begin{aligned} & \mathbb{E}_{\epsilon} \epsilon_i \epsilon_k^\top \epsilon_l \epsilon_j^\top \\ &= \mathbb{E}_{\epsilon} \epsilon_i \epsilon_i^\top \epsilon_i \epsilon_j^\top \\ &= \mathbb{E}_{\epsilon_i} \epsilon_i \epsilon_i^\top \epsilon_i \mathbb{E}_{\epsilon_j} \epsilon_j^\top \\ &= \mathbf{0} \end{aligned}$$

(II.2.c) if $l = j$,

$$\begin{aligned} & \mathbb{E}_{\epsilon} \epsilon_i \epsilon_k^\top \epsilon_l \epsilon_j^\top \\ &= \mathbb{E}_{\epsilon_i, \epsilon_j} \epsilon_i \epsilon_i^\top \epsilon_j \epsilon_j^\top \\ &= \mathbb{E}_{\epsilon_i} [\epsilon_i \epsilon_i^\top] \mathbb{E}_{\epsilon_j} [\epsilon_j \epsilon_j^\top] \\ &= \sigma^4 I_d \end{aligned}$$

(II.3) $k = j$,

(II.3.a) if $l \neq i, l \neq j$. Again similar to (II.1) by swapping k and j and $\mathbb{E}_{\epsilon} \epsilon_i \epsilon_k^\top \epsilon_l \epsilon_j^\top = \mathbf{0}$.

(II.3.b) if $l = i$. By swapping the position, we have

$$\begin{aligned} & \mathbb{E}_{\epsilon} \epsilon_i \epsilon_k^\top \epsilon_l \epsilon_j^\top \\ &= \mathbb{E}_{\epsilon_i, \epsilon_j} \epsilon_i (\epsilon_j^\top \epsilon_i) \epsilon_j^\top \\ &= \mathbb{E}_{\epsilon_i, \epsilon_j} \epsilon_i (\epsilon_i^\top \epsilon_j) \epsilon_j^\top \\ &= \mathbb{E}_{\epsilon_i} [\epsilon_i \epsilon_i^\top] \mathbb{E}_{\epsilon_j} [\epsilon_j \epsilon_j^\top] \\ &= \sigma^4 I_d \end{aligned}$$

(II.3.c) $l = j$.

$$\begin{aligned} & \mathbb{E}_{\epsilon} \epsilon_i \epsilon_k^\top \epsilon_l \epsilon_j^\top \\ &= \mathbb{E}_{\epsilon} \epsilon_i \epsilon_j^\top \epsilon_j \epsilon_j^\top \\ &= \mathbb{E}_{\epsilon_i} \epsilon_i \mathbb{E}_{\epsilon_j} \epsilon_j^\top \epsilon_j \epsilon_j^\top \\ &= \mathbf{0} \end{aligned}$$

As a result, when we have $i \neq j$, the total sum over all the cases (II.1) - (II.3) is

$$\sum_{k=1}^n \sum_{l=1}^n \mathbb{E}_{\epsilon} \epsilon_i \epsilon_k^\top \epsilon_l \epsilon_j^\top = 2\sigma^4 I_d \quad (64)$$

End of all Cases.

Using the result in (63) and (64), we see that for the fixed time step t ,

$$\mathbb{E}_{\{\epsilon\}|\tau=t-1} \|\text{GPES}_{K=c}(\theta)\|_2^2 \quad (65)$$

$$= \frac{1}{\sigma^4} \left(\sum_{i=1}^n (nd+2) \sigma^4 \|a_i\|_2^2 + \sum_{i \neq j} 2\sigma^4 a_i^\top a_j \right) \quad (66)$$

$$= \sum_{i=1}^n (nd+2) \|a_i\|_2^2 + \sum_{i \neq j} 2a_i^\top a_j \quad (67)$$

$$= \left(\sum_{i=1}^n (d+2) \|a_i\|_2^2 + \sum_{i=1}^n (n-1)d \|a_i\|_2^2 \right) + \left(\sum_{i \neq j} (d+2) [a_i]^\top a_j - \sum_{i \neq j} d a_i^\top a_j \right) \quad (68)$$

$$= \left(\sum_{i=1}^n (d+2) \|a_i\|_2^2 + \sum_{i \neq j} (d+2) [a_i]^\top a_j \right) + \left(\sum_{i=1}^n (n-1)d \|a_i\|_2^2 - \sum_{i \neq j} d [a_i]^\top a_j \right) \quad (69)$$

$$= (d+2) \left\| \sum_{i=1}^n a_i \right\|_2^2 + \frac{d}{2} \left(\sum_{i=1}^n 2(n-1) \|a_i\|_2^2 - \sum_{i \neq j} 2a_i^\top a_j \right) \quad (70)$$

$$= (d+2) \left\| \sum_{i=1}^n a_i \right\|_2^2 + \frac{d}{2} \left(\sum_{i=1}^n (n-1) \|a_i\|_2^2 + \sum_{j=1}^n (n-1) \|a_j\|_2^2 - \sum_{i \neq j} 2a_i^\top a_j \right) \quad (71)$$

$$= (d+2) \left\| \sum_{i=1}^n a_i \right\|_2^2 + \frac{d}{2} \left(\sum_{i=1}^n \sum_{j \neq i} \|a_i\|_2^2 + \sum_{j=1}^n \sum_{i \neq j} \|a_j\|_2^2 - \sum_{i \neq j} 2a_i^\top a_j \right) \quad (72)$$

$$= (d+2) \left\| \sum_{i=1}^n a_i \right\|_2^2 + \frac{d}{2} \left(\sum_{i=1, j=1, i \neq j}^n \|a_i\|_2^2 + \|a_j\|_2^2 - 2a_i^\top a_j \right) \quad (73)$$

$$= (d+2) \left\| \sum_{i=1}^n a_i \right\|_2^2 + \frac{d}{2} \sum_{i=1, j=1, i \neq j}^n \|a_i - a_j\|_2^2 \quad (74)$$

Now we substitute a_i with $g_{c,i}^t$ and n back with $\lceil t/c \rceil$, we have

$$\mathbb{E}_{\{\epsilon\}|\tau=t-1} \|\text{GPES}_{K=c}(\theta)\|_2^2 \quad (75)$$

$$= (d+2) \left\| \sum_{i=1}^{\lceil t/c \rceil} g_{c,i}^t \right\|_2^2 + \frac{d}{2} \sum_{i=1, j=1, i \neq j}^{\lceil t/c \rceil} \|g_{c,i}^t - g_{c,j}^t\|_2^2 \quad (76)$$

$$= (d+2) \|g^t\|_2^2 + \frac{d}{2} \sum_{j=1, j'=1}^{\lceil t/c \rceil} \|g_{c,j}^t - g_{c,j'}^t\|_2^2 \quad (77)$$

This completes the derivation for ①.

② Expressing $\|\mathbb{E} \text{GPES}_{K=c}(\theta)\|_2^2$

This amounts to computing the expectation of the $\text{GPES}_{K=c}(\theta)$ estimator:

$$\mathbb{E} \text{GPES}_{K=c}(\theta) \quad (78)$$

$$= \mathbb{E}_{\tau} \mathbb{E}_{\epsilon} \text{GPES}_{K=c}(\theta) \quad (79)$$

$$= \frac{1}{T} \sum_{t=1}^T \mathbb{E}_{\epsilon|\tau=t-1} \text{GPES}_{K=c}(\theta) \quad (80)$$

$$= \frac{1}{T} \sum_{t=1}^T \frac{1}{\sigma^2} \mathbb{E}_{\epsilon} \sum_{j=1}^{\lceil t/c \rceil} \left(\sum_{i=1}^{\lceil t/c \rceil} \epsilon_i \right) \epsilon_j^{\top} g_{c,j}^t \quad (81)$$

$$= \frac{1}{T} \sum_{t=1}^T \frac{1}{\sigma^2} \sum_{j=1}^{\lceil t/c \rceil} \sum_{i=1}^{\lceil t/c \rceil} \mathbb{E}_{\epsilon} [\epsilon_i \epsilon_j^{\top}] g_{c,j}^t \quad (82)$$

$$= \frac{1}{T} \sum_{t=1}^T \frac{1}{\sigma^2} \sum_{j=1}^{\lceil t/c \rceil} \sigma^2 g_{c,j}^t \quad (83)$$

$$= \frac{1}{T} \sum_{t=1}^T \sum_{j=1}^{\lceil t/c \rceil} g_{c,j}^t \quad (84)$$

$$= \frac{1}{T} \sum_{t=1}^T g^t \quad (85)$$

Thus we have

$$\|\mathbb{E} \text{GPES}_{K=c}(\theta)\|_2^2 = \left\| \frac{1}{T} \sum_{t=1}^T g^t \right\|_2^2. \quad (86)$$

This completes the derivation for ②.

Combining the result we have for ① (Equation (77)) and ② (Equation (86)), we have

$$\begin{aligned} & \text{tr}(\text{Cov}[\text{GPES}_{K=c}(\theta)]) \\ &= \frac{1}{T} \sum_{t=1}^T \mathbb{E}_{\{\epsilon_i\}|\tau=t-1} \|\text{GPES}_{K=c}(\theta)\|_2^2 - \|\mathbb{E} \text{GPES}_{K=c}(\theta)\|_2^2 \\ &= \frac{(d+2)}{T} \sum_{t=1}^T (\|g^t\|_2^2) - \left\| \frac{1}{T} \sum_{t=1}^T g^t \right\|_2^2 + \frac{1}{T} \sum_{t=1}^T \left(\frac{d}{2} \sum_{j=1, j'=1}^{\lceil t/c \rceil} \|g_{c,j}^t - g_{c,j'}^t\|_2^2 \right) \end{aligned}$$

This completes the proof for Theorem 5. □

C.5 Proof of Corollary 6

Corollary 6. *Under Assumption 2, when $W = 1$, the gradient estimator $\text{GPES}_{K=T}(\theta)$ has the smallest total variance among all $\{\text{GPES}_K : K \in [T]\}$ estimators.*

Proof. We notice that in Equation 9, the only term that depends on c is the third term:

$$\frac{1}{T} \sum_{t=1}^T \left(\frac{d}{2} \sum_{j=1, j'=1}^{\lceil t/c \rceil} \|g_{c,j}^t - g_{c,j'}^t\|_2^2 \right). \quad (87)$$

This term can be made zero by having $c = T$: in this case, $\lceil t/T \rceil = 1$ for any $t \in [T]$, hence there is only one $g_{T,1}^t$ to compare against itself. Thus having $c = T$ minimizes the total variance among the class of $\text{GPES}_{K=c}$ estimators. \square

C.6 Proof of Corollary 7

Corollary 7. *Under Assumption 2, when W divides T , the NRES gradient estimator has the smallest total variance among all $\text{GPES}_{K=cW}$ estimators $c \in \mathbb{Z} \cap [1, T/W]$.*

Proof. Here the key idea is that because W divides T , we can define a mega unrolled computation graph and apply Corollary 6.

Specifically, we consider a mega UCG where the inner state is represented by all the states within a size W truncation window. The total horizon length of this mega UCG is $T' = T/W$. The initial state of the mega UCG is given by

$$S_0 := (s_0, \dots, s_0) \in \mathbb{R}^{Wp}. \quad (88)$$

For time step $t' \in \{1, \dots, T/W\}$ in this mega UCG, the mega-state $S_{t'}$ is given by the concatenation of all the states in a given original truncation window

$$S_{t'} := (s_{(t'-1) \cdot W + 1}, \dots, s_{t' \cdot W}) \in \mathbb{R}^{Wp}, \quad (89)$$

The learnable parameter in this problem is still $\theta \in \mathbb{R}^d$. The transition dynamics $u_{t'} : \mathbb{R}^{Wp} \times \mathbb{R}^d \rightarrow \mathbb{R}^{Wp}$ works as follows:

$$u_{t'} : \left(S_{t'} = \begin{bmatrix} s_{(t'-1) \cdot W + 1} \\ s_{(t'-1) \cdot W + 2} \\ \vdots \\ s_{t' \cdot W} \end{bmatrix}, \theta \right) \mapsto S_{t'+1} := \begin{bmatrix} f_{t'W+1}(s_{t' \cdot W}, \theta) \\ f_{t'W+2}(f_{t'W+1}(s_{t' \cdot W}, \theta), \theta) \\ \vdots \\ f_{(t'+1)W}(\dots(f_{t'W+2}(f_{t'W+1}(s_{t' \cdot W}, \theta), \theta), \theta), \dots, \theta). \end{bmatrix} \quad (90)$$

Here, the mega transition only look at the last time step's original state in $S_{t'}$ and unroll it forwards W steps to form the next mega state.

The mega loss function for step t' is defined as $\ell_{t'}^s : \mathbb{R}^{Wp} \rightarrow \mathbb{R}$:

$$\ell_{t'}^s((s_{(t'-1) \cdot W + 1}, \dots, s_{t' \cdot W})) = \frac{1}{W} \sum_{i=1}^W L_{(t'-1)W+i}^s(s_{(t'-1)W+i}), \quad (91)$$

which simply averages each original inner state's loss within the truncation window.

Here, when we consider a truncation window of size W in the original graph, it is equivalent to a truncation window of size 1 in the mega UCG. To apply Corollary 6 to this graph, we only need to make sure Assumption 2 holds for this mega graph. Here we see that, by Assumption 2 on this original graph, we have

$$\begin{aligned}
& \ell_{t'}(\theta + v_1, \dots, \theta + v_{t'}) - \ell_{t'}(\theta - v_1, \dots, \theta - v_{t'}) \\
&= \frac{1}{W} \sum_{j=1}^W [L_{W(t'-1)+j}([\theta + v_1]_{\times W}, \dots, [\theta + v_{t'}]_{\times j}) - L_{W(t'-1)+j}([\theta - v_1]_{\times W}, \dots, [\theta - v_{t'}]_{\times j})] \\
&= \frac{1}{W} \sum_{j=1}^W 2 \sum_{i'=1}^{t'} [v_{i'}]^\top g_{W,i'}^{W(t'-1)+j} \\
&= 2 \sum_{i'=1}^{t'} [v_{i'}]^\top \left(\frac{1}{W} \sum_{j=1}^W g_{W,i'}^{W(t'-1)+j} \right)
\end{aligned}$$

Thus for this mega graph, the set of vectors satisfying Assumption 2 is $g_{i'}^{t'} = \left(\frac{1}{W} \sum_{j=1}^W g_{W,i'}^{W(t'-1)+j} \right)$.

With the mega graph satisfying the assumption in Corollary 6, we see that when the truncation window is of size 1 in the mega graph, the gradient estimator NRES on this mega graph has smaller trace of covariance than other $\text{GPES}_K = c$ estimators on this mega graph. Here, running NRES on the mega-graph is equivalent to running NRES on the original graph, while the gradient estimator $\text{GPES}_K = c$ on the mega-graph is equivalent to the gradient estimator $\text{GPES}_{K=cW}$ on the original UCG. Thus we have proved that the NRES gradient estimator on the original graph has the smallest total variance among all $\text{GPES}_{K=cW}$ estimators, thus completing the proof.

□

C.7 Proof of Theorem 8

Theorem 8. Under Assumption 2, for any W that divides T , if

$$\sum_{k=1}^{T/W} \left\| \sum_{t=W \cdot (k-1)+1}^{W \cdot k} g^t \right\|_2^2 \leq \frac{d+1}{d+2} \left\| \sum_{j=1}^{T/W} \sum_{t=W \cdot (j-1)+1}^{W \cdot j} g^t \right\|_2^2, \quad (92)$$

then $\text{tr}(\text{Cov}(\frac{1}{T/W} \sum_{i=1}^{T/W} \text{NRES}_i(\theta))) \leq \text{tr}(\text{Cov}(\text{FullES}(\theta)))$ where $\text{NRES}_i(\theta)$ are iid NRES estimators.

Proof. We first analytically express the FullES gradient estimator. Under the Assumption 2,

$$\text{FullES}(\theta) \quad (93)$$

$$= \frac{1}{2\sigma^2} [L([\theta + \epsilon]_{\times T}) - L([\theta - \epsilon]_{\times T})] \epsilon \quad (94)$$

$$= \frac{1}{\sigma^2} \epsilon \epsilon^\top \left(\frac{1}{T} \sum_{t=1}^T g^t \right) \quad (95)$$

Because $\mathbb{E}_\epsilon \epsilon \epsilon^\top \epsilon \epsilon^\top = (d+2)\sigma^2 I_{d \times d}$, we can see that

$$\text{tr}(\text{Cov}[\text{FullES}(\theta)]) = (d+2) \left\| \frac{1}{T} \sum_{t=1}^T g^t \right\|_2^2 - \left\| \frac{1}{T} \sum_{t=1}^T g^t \right\|_2^2 \quad (96)$$

$$= (d+1) \left\| \frac{1}{T} \sum_{t=1}^T g^t \right\|_2^2 \quad (97)$$

From Theorem 5 and Corollary 7, we can see that the trace of covariance for a single NRES when $W \geq 1$ is given by

$$\text{tr}(\text{Cov}(\text{NRES}(\theta))) = \frac{(d+2)}{T/W} \sum_{k=1}^{T/W} \left(\left\| \frac{1}{W} \sum_{t=W \cdot (k-1)+1}^{W \cdot k} g^t \right\|_2^2 \right) - \left\| \frac{1}{T} \sum_{t=1}^T g^t \right\|_2^2 \quad (98)$$

Thus the trace of covariance of T/W iid NRES workers' trace of covariance scales with $\frac{1}{T/W}$:

$$\text{tr}(\text{Cov}(\frac{1}{T/W} \sum_{i=1}^{T/W} \text{NRES}_i(\theta))) \quad (99)$$

$$= \frac{1}{T/W} \text{tr}(\text{Cov}(\text{NRES}(\theta))) \quad (100)$$

$$= \frac{1}{T/W} \frac{(d+2)}{T/W} \frac{1}{W^2} \sum_{k=1}^{T/W} \left(\left\| \sum_{t=W \cdot (k-1)+1}^{W \cdot k} g^t \right\|_2^2 \right) - \frac{1}{T/W} \left\| \frac{1}{T} \sum_{t=1}^T g^t \right\|_2^2 \quad (101)$$

$$\leq \frac{(d+2)}{T^2} \sum_{k=1}^{T/W} \left(\left\| \sum_{t=W \cdot (k-1)+1}^{W \cdot k} g^t \right\|_2^2 \right) \quad (102)$$

$$\leq \frac{(d+2)}{T^2} \frac{d+1}{d+2} \left\| \sum_{k=1}^{T/W} \sum_{t=W \cdot (k-1)+1}^{W \cdot k} g^t \right\|_2^2 \quad (\text{using the condition in Theorem 8}) \quad (103)$$

$$= \frac{(d+1)}{T^2} \left\| \sum_{k=1}^{T/W} \sum_{t=W \cdot (k-1)+1}^{W \cdot k} g^t \right\|_2^2 \quad (104)$$

$$= \frac{(d+1)}{T^2} \left\| \sum_{t=1}^T g^t \right\|_2^2 \quad (105)$$

$$= (d+1) \left\| \frac{1}{T} \sum_{t=1}^T g^t \right\|_2^2 \quad (106)$$

$$= \text{tr}(\text{Cov}[\text{FulES}(\theta)]) \quad (107)$$

This completes the proof.

□

D Experiment Details

In this section, we first describe the tuned hyperparameters for each of the three tasks. We then supplement Figure 6(a) with further comparison of the top three gradient estimators for the meta-training learned optimizer application. We finally describe the computation resources needed to run these experiments.

D.1 Hyperparameters

D.1.1 Learning dynamical system parameters

In the Lorenz system parameter learning task, we use the vanilla SGD optimizer to update the parameter $\theta = (\ln(a), \ln(r))$ starting at $\theta_{\text{init}} = (\ln(a), \ln(r)) = (3.116, 3.7)$ with the episode length at $T = 2000$.

- For offline methods, we use only $N = 1$ worker for BPTT to compute the non-smoothed true gradient since we only have one example sequence to learn from. We use $N = 10$ workers for FullES, which is $T/W = 20$ times less than the number of workers used by NRES.
- For all the online methods, we use $N = 200$ workers and a truncation window of size $W = 100$. This relationship exactly matches the condition considered in Theorem 8, and the total amount of computation for FullES and NRES to produce one gradient estimate is roughly the same.
- For all the ES methods, we use the smoothing standard deviation $\sigma = 0.04$.

For each gradient estimation methods, we tune its SGD constant learning rate from the following set

$$\{10^{-3}, 3 \times 10^{-4}, 10^{-4}, 3 \times 10^{-5}, 10^{-5}, 10^{-6}, 10^{-7}, 10^{-8}, 10^{-9}, 10^{-10}, 10^{-11}, 10^{-12}, 10^{-13}\}. \quad (108)$$

Here we choose the learning rate to ensure that **1**) there is no NaN in gradients/loss value due to the exploding gradient from the chaotic loss surface; **2**) the learning rate doesn't result in a significant increase in the loss. The learning rate range is made so wide because for all the unbiased AD methods, *these two issues would occur unless we use a trivially small learning rate*. Among the learning rates that pass these two requirements, we choose the best learning rate such that the optimization metric of interest decreases the fastest. For each method, the tuned learning rate used for Figure 4(a) is given in Table 5.

Table 4: Learning rates (schedules) used for different gradient estimators on the Lorenz system parameter learning task

method name	SGD learning rate (schedule)
BPTT $N = 1$	10^{-8}
TBPTT $N = 200, W = 100$	3×10^{-4}
DODGE $N = 200, W = 100$	10^{-10}
UORO $N = 200, W = 100$	10^{-13}
FullES $N = 10$	3×10^{-5}
TES $N = 200, W = 100$	3×10^{-4}
PES $N = 200, W = 100$	10^{-5} for the first 1000 updates; 10^{-6} afterwards
NRES $N = 200, W = 100$	10^{-5}

As PES couldn't afford to use the same learning rate as NRES because of the unstable convergence (see Figure 4(b)), we hand-tuned a learning rate decay schedule for PES to maximally allow for its convergence.

To generate Figure 4(b), we use a constant SGD learning rate of 10^{-5} to isolate the variance properties of different GPES_K estimators.

D.1.2 Meta-training learned optimizers

The inner problem model is a three-layer MLP with GeLU activation [Hendrycks and Gimpel, 2016] with dimension of 32 for each hidden layer. We choose GeLU instead of ReLU because GeLU is infinitely differentiable. By this design choice, the meta-training loss function is infinitely differentiable with respect to θ . We downsize the dataset Fashion MNIST [Xiao et al., 2017] to 8 by 8 images to make both the unrolled computation graph small enough to fit onto a single GPU and also to make training fast. We split the Fashion MNIST training’s first 80% image for inner problem training and the last 20% images for inner problem validation. During the inner training, we randomly sample a training batch of size 128 to compute the training gradient using the cross entropy loss. After updating the inner model with the learned optimizer, we evaluate the meta-loss (our objective) using cross entropy on a randomly sampled validation batch of size 128. One inner problem training lasts $T = 1000$ steps of updates using the learned optimizer.

- For offline methods, because we fix the data sequence in inner training and inner evaluation, we only need $N = 1$ for BPTT to compute the gradient exactly. For FulLES, we tuned its number of workers among the set $N \in \{1, 3, 10\}$.
- For all the online methods, we use the smallest possible truncation window size of $W = 1$ to test the online algorithms to the extreme. We use a total of $N = 100$ workers for all the online method. Therefore, to produce one gradient update, an online worker only runs $N \cdot W/T = 100 \cdot 1/1000 = 10\%$ of an episode.
- For all the ES methods, we use the smoothing standard deviation at $\sigma = 0.01$.

When meta-training the learned optimizer, we use Adam with the default parameters (other than a tuneable learning rate) to optimize the meta-training loss. For each gradient estimation method, we tune the learning rate in the following range

$$\{3 \times 10^{-2}, 1 \times 10^{-2}, 3 \times 10^{-3}, 10^{-3}, 3 \times 10^{-4}, 10^{-4}, 3 \times 10^{-5}\} \quad (109)$$

Table 5: Learning rates used for different gradient estimators on the meta-training learned optimizer task

method name	Adam learning rate (schedule)
BPTT $N = 1$	3×10^{-4}
TBPTT $N = 100, W = 1$	10^{-2}
DODGE $N = 100, W = 1$	10^{-5}
UORO $N = 100, W = 1$	3×10^{-5}
FulLES $N = 10$	3×10^{-2}
TES $N = 100, W = 1$	10^{-3}
PES $N = 100, W = 1$	3×10^{-4}
GPES_K $N = 100, W = 1, K = 4$	3×10^{-4}
GPES_K $N = 100, W = 1, K = 16$	3×10^{-4}
GPES_K $N = 100, W = 1, K = 64$	3×10^{-4}
GPES_K $N = 100, W = 1, K = 256$	3×10^{-4}
NRES $N = 100, W = 1$	3×10^{-4}

After choosing a learning rate for a particular method over a specific random seed, we also check its performance on another seed to ensure its consistency (otherwise we lower the learning rate and try again). For each method, the best learning rate is given in Table 5.

D.1.3 Reinforcement Learning

We use the default Mujoco tasks Swimmer-v4 and Half Cheetah-v4 from Open AI gym (gymnasium version) [Brockman et al., 2016]. The tasks have a horizon length of $T = 1000$ without any half-way resets due to dangerous positions. Here, following [Mania et al., 2018], we learn a deterministic linear policy that maps the observation space to the action space: for Swimmer-v4, this amounts to mapping an 8-dimensional observation space to a 2-dimensional action space ($d = 2 \times 8 = 16$), while for Half Cheetah-v4, this amounts to mapping a 17-dimensional observation space to a 6-dimensional action space ($d = 6 \times 17 = 102$). Because we can't differentiate through the dynamics, we only consider ES methods for this task.

- For the online ES methods on both tasks, we fix the truncation window size at $W = 100$. For the Swimmer task, We use $N = 30$ workers for online ES methods and $N = 3$ for FullES. For the Half Cheetah task, We use $N = 100$ workers for online ES workers and $N = 10$ workers for FullES. These choices for both tasks ensure that the number of environment steps used by all methods in each gradient update are roughly comparable.
- We choose $\sigma = 0.3$ for Swimmer-v4 and $\sigma = 0.004$ for Half Cheetah-v4 as it performs well for FullES.

For Swimmer-v4, we tune the learning rate used by the SGD algorithm in the following range:

$$\{10^2, 3 \times 10^1, 10^1, 3 \times 10^0, 10^0, \}$$
 (110)

For Half Cheetah-v4, we tune the learning rate used by the SGD algorithm in the following range:

$$\{10^{-4}, 3 \times 10^{-5}, 10^{-5}, \}$$
 (111)

The chosen learning rates for each method are given in Table 6 and Table 7.

Table 6: Learning rates used for different gradient estimators on the Mujoco Swimmer-v4 task

method name	SGD learning rate
FullES $N = 3$	1×10^0
TES $N = 30, W = 100$	3×10^1
PES $N = 30, W = 100$	1×10^0
NRES $N = 30, W = 100$	3×10^0

Table 7: Learning rates used for different gradient estimators on the Mujoco Half Cheetah-v4 task

method name	SGD learning rate
FullES $N = 10$	3×10^{-5}
TES $N = 100, W = 100$	3×10^{-5}
PES $N = 100, W = 100$	3×10^{-5}
NRES $N = 100, W = 100$	3×10^{-5}

D.2 Additional Comparisons on the Learned Optimizers application

In Figure 6(a), we have shown that NRES can achieve a faster minimization of the nonsmoothed training loss than other gradient estimators in the first 2500 seconds of optimization. Here we further compare the top three methods (NRES, PES, and FullES) by allowing the methods to train longer in Figure 8. We see that to reach the loss value NRES reaches in 700 seconds, PES and NRES take more than 5 and 10 times the amount of time respectively. This further demonstrates the advantage of NRES for effective optimization.

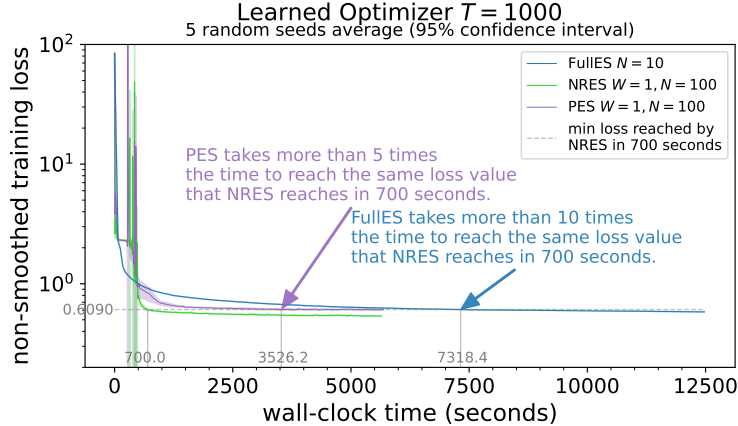


Figure 8: We compare the top three gradient estimators in the meta-training learned optimizer task introduced in Section 6.2 by allowing each method to train for a longer period of time than shown in Figure 6. We notice that PES and NRES takes more than 5 and 10 times (respectively) longer than NRES to reach the loss value NRES reaches in an early stage of training (700 seconds).

D.3 Computation resource needed

To ensure we can tune the hyperparameters for each gradient estimation methods well (as described in the Section D.1), we keep our problem size at a reasonable size. For any gradient estimation method on any of the three tasks, we can train on a single machine with a single GPU using memory less than 10GB. As shown in the Figure 5 (Lorenz) and Figure 6(a) (Learned optimizer), NRES can converge in wall-clock time in less than 300 and 2500 seconds respectively. For the Swimmer-v4 RL and Half Cheetah-v4 task, because the environment transitions are computed on CPUs in OpenAI Gym, we can run the entire experiment on CPU and it takes less than 2 hours and 24¹⁴ hours respectively to finish training for all the ES methods. We believe these tasks are valuable experiment set ups to analyze new online Evolution Strategies methods in the future.

D.4 Experiment implementation

We build our codebase following the high level logic in the codebase by [Metz et al., 2022b]. We provide the implementation for all the algorithms used in this paper in JAX at <https://github.com/OscarcarLi/Noise-Reuse-Evolution-Strategies>.

¹⁴In fact, only TES would require more than 6 hours on Half Cheetah because of its requirement of an immutable inner state implementation.